Dynamic Output Controllers for Exponential Stabilization of Periodic Orbits for Multi-Domain Hybrid Models of Robotic Locomotion

Kaveh Akbari Hamed*

Assistant Professor Mechanical Engineering Virginia Tech Blacksburg, VA 24061

Email: kavehakbarihamed@vt.edu

Bita Safaee

Ph.D. Student
Mechanical Engineering
Virginia Tech
Blacksburg, VA 24061
Email: bsafaee@vt.edu

Robert D. Gregg

Associate Professor
Department of Electrical Engineering and Computer Science and Robotics Institute
University of Texas at Dallas
Richardson, TX 75080
Email: rgregg@utdallas.edu

The primary goal of this paper is to develop an analytical framework to systematically design dynamic output feedback controllers that exponentially stabilize multi-domain periodic orbits for hybrid dynamical models of robotic locomotion. We present a class of parameterized dynamic output feedback controllers such that (1) a multi-domain periodic orbit is induced for the closed-loop system, and (2) the orbit is invariant under the change of the controller parameters. The properties of the Poincaré map are investigated to show that the Jacobian linearization of the Poincaré map around the fixed point takes a triangular form. This demonstrates the nonlinear separation principle for hybrid periodic orbits. We then employ an iterative algorithm based on a sequence of optimization problems involving bilinear matrix inequalities to tune the controller parameters. A set of sufficient conditions for the convergence of the algorithm to stabilizing parameters is presented. Full state stability and stability modulo yaw under dynamic output feedback control are addressed. The power of the analytical approach is ultimately demonstrated through designing a nonlinear dynamic output feedback controller for walking of a 3D humanoid robot with 18 state variables and 325 controller parameters.

Nomenclature

- Λ , V, \mathcal{E} Graph of the hybrid model, set of vertices, set of edges
- X, U, D State space, admissible controls set, domain of admissibility

- Δ , S Discrete-time dynamics, guards of the hybrid system
- x,u,y,x^*,u^* State variables, control inputs, measurable outputs, nominal state variables, nominal control inputs
- (f,g,h) Vector fields for continuous-time dynamics s Switching function
- μ, T^{\star} Next domain function, fundamental period
- $(\cdot)_{\nu},(\cdot)_{\nu\to\mu(\nu)}$ Variables for the continuous-time domain ν , variables for the discrete-time transition $\nu\to\mu(\nu)$
- $(\cdot)^-,(\cdot)^+$ Variables right before and after the discrete transition
- T Discrete set of switching times
- \hat{x}, \hat{y} Estimated state variables, estimated outputs
- z, Γ Controlled functions, state feedback law
- ξ, η, H, L Controller parameters, observer parameters, output matrix, observer gain
- Ξ Set of admissible controller parameters
- n, m, ζ Number of state variables, controls, and outputs
- p_c, p_o Number of controller and observer parameters
- e,ω,Ω Estimation error, continuous-time dynamics of the error, discrete-time dynamics of the error
- φ , T State solution, time-to-switching function
- $(\cdot)_a$ Augmented variables
- $(\cdot)_x, (\cdot)_e$ Variables corresponding to the state variables x, variables corresponding to the estimation error e
- $(\cdot)^{\text{ol}}, (\cdot)^{\text{cl}}$ Open-loop and closed-loop variables
- P,A Poincaré map, Jacobian linearization of the Poincaré map

^{*}Corresponding Author

- N, ρ Number of vertices and executed sequence of vertices on the graph
- Π,Φ,J,D Saltation matrix, trajectory sensitivity matrix, Jacobian linearization of continuous-time dynamics, Jacobian linearization of discrete-time dynamics
- $(\cdot)^*$ Periodic orbit variables
- $(\cdot)_{11}, (\cdot)_{22}$ Variables for the controller synthesis, variables for the observer synthesis
- W, γ, δ Decision variables for the BMI optimization
- $\Delta \xi, \Delta \eta$ Increment in controller and observer parameters
- \hat{A} , Approximate Jacobian matrix, convex hull of Jacobian matrices

1 Introduction

This paper presents an analytical foundation to synthesize dynamic output feedback controllers that exponentially stabilize periodic orbits for multi-domain hybrid dynamical systems of robotic locomotion. We consider a general family of parameterized dynamic output feedback controllers with full-order observer portions. Based on the Poincaré sections analysis, this paper extends the nonlinear separation principle to the stabilization problem of multi-domain hybrid periodic orbits. We use an approach based on an iterative sequence of optimization problems involving bilinear and linear matrix inequalities (BMIs and LMIs) to tune the state feedback and observer parameters. The convergence of the algorithm to a set of stabilizing parameters at a finite number of iterations is addressed. The framework can ameliorate particular challenges in the design of dynamic output feedback controllers for increasingly sophisticated legged robots with high dimensionality, underactuation, and hybrid nature.

1.1 Motivation

Knowing the system state is necessary to solve many nonlinear control theory problems, e.g., feedback linearization. In the case of legged locomotion, dynamic output feedback control is desirable for several reasons. Although legged robots are becoming more mechanically sophisticated with higher degrees of freedom (DOFs), state-of-the-art nonlinear control approaches cannot deal with possible encoder failures. In addition, the lack of velocity sensors is a ubiquitous problem in the design of state feedback controllers for legged machines. Numerical differentiation to extract velocity components of legged robots is well known to be an ill-conditioned problem in the sense that small perturbations on encoder measurements may induce large changes in the derivatives [1]. In particular, the velocity components of legged robots may go under abrupt changes according to the contacts of the feet with the walking surface. Consequently, the position profiles over the infinitesimal periods of rigid impacts is continuous, but not continuously differential. More specifically, the velocity components right before and after the impact are not same. Finally, it is not clinically feasible for human users of prosthetic legs to wear sensors at their intact joints. This underlines the need to systematically develop dynamic output feedback controllers to stabilize gaits for models of autonomous and rehabilitation legged machines with high degrees of freedom, underactuation, and a limited set of available measurements.

1.2 Related Work for Legged Locomotion

Hybrid systems exhibit characteristics of both continuous- and discrete-time dynamical systems [2, 3, 4, 5] and have become a very powerful approach to study legged locomotion and mechanical systems subject to impacts [6,7]. Models of legged robots are hybrid with continuous-time domains representing the Lagrangian dynamics and discrete-time transitions representing the changes in physical constraints (i.e., a nonstance leg contacting the walking Steady-state robotic locomotion corresponds surface). to periodic solutions of these hybrid models. State-ofthe-art nonlinear control approaches for robotic walking such as the zero moment point (ZMP) criterion [8, 9], controlled symmetries [10], hybrid reduction [11, 12], transverse linearization [13], and hybrid zero dynamics (HZD) [14, 15, 16] assume that all state variables are available for feedback in real time. The ZMP criterion supposes full actuation and generates time trajectories to be tracked for quasi-static and flat-footed walking. Feedback control algorithms that directly deal with the hybrid nature of legged locomotion have come out of controlled symmetries, hybrid reduction, transverse linearization, and HZD. Controlled symmetries and hybrid reduction typically assume full actuation and make use of potential energy and Lagrangian shaping, respectively. However, transverse linearization and HZD-based controllers are the only controllers of the abovementioned methods that explicitly deal with general cases of underactuation. HZD-based controllers have been validated numerically and experimentally for (i) 2D and 3D bipedal robots, including RABBIT [17, 18], MABEL [19, 20, 21], ERNIE [22], AMBER [23], ATRIAS [24, 25, 26, 27], and DURUS [28, 29] prototypes, (ii) powered prosthetic legs [30, 31, 32, 33], (iii) exoskeletons [34], (iv) monopedal robots [35, 36], and (v) quadruped robots [37]. In the HZD approach, a set of output functions, referred to as virtual constraints, is defined for the continuous-time dynamics of the system and asymptotically driven to zero by partial linearizing feedback controllers [38].

1.3 Related Work for Observer Design

State-of-the-art observer design approaches for nonlinear dynamical systems pertain to the estimation of state variables around equilibrium points and not hybrid periodic orbits. The design of an observer for nonlinear dynamical systems is a significant challenge. This challenge has been addressed in the literature of dynamical systems through the development of different techniques including Luenberger-like observers [39, 40, 41], the use of LMIs [39, 40, 42] and BMIs [43, 44, 45], and the use of high-gain observers [46, 47, 48, 49]. The separation principle has also been extended to the stabilization problem of equilibrium points for nonlinear systems. In particular, this has been done for Lips-

chitz nonlinear systems [40], circle-criterion-based observer design approaches [41], high-gain observers [46], feedback linearization-based observer design techniques [50], variable design methodology [51], globally Lipschitz systems [52], global stabilizable and observable systems [53], uniformly completely observable systems [54], modified circlecriterion-based observer design techniques [55], and systems with incremental quadratic inequality [56]. Asymptotic observers that deal with periodic orbits of underactuated bipedal robots have been designed based on two different approaches. The first approach employs sliding mode observers to estimate the absolute orientation of planar bipedal robots when the robot's shape (i.e., internal joint) variables are measurable [57, 58, 59]. The second approach makes use of high gain full- and reduced-order observers to estimate generalized velocity components when position variables are measurable [60]. However, these approaches cannot address the general problem of designing observer-based output feedback controllers for a given set of measurements.

1.4 Challenges

The most basic tool to investigate the stability of hybrid periodic orbits is the method of Poincaré sections [61, 4, 16, 62, 26] that describes the evolution of the hybrid system on a hyperplane transversal to the orbit by a discrete-time system, referred to as the Poincaré return map. One drawback of Poincaré sections analysis is the lack of a closed-form expression for the Poincaré map and its Jacobian linearization, which complicates the design of continuous-time controllers for hybrid models of legged robots. To tackle this problem, we have recently presented an iterative algorithm based on BMI optimizations to choose stabilizing state feedback laws from a family of parameterized controllers [25, 33, 63]. This algorithm was numerically and experimentally verified to design centralized [64, 65] as well as decentralized controllers [33] for hybrid models of biped robots. However, there is not any systematic algorithm to design observer-based output feedback controllers for these increasingly sophisticated machines. We would like to present an analytical foundation to extend the BMI algorithm for the design of dynamic output feedback controllers that exponentially stabilize given hybrid periodic orbits.

1.5 Goals, Objectives, and Contributions

The *primary goal* of this paper is to present an analytical foundation to systematically design dynamic output feedback controllers that stabilize underactuated gaits for high-dimensional and multi-domain hybrid models of legged locomotion. This goal will be achieved through the following *objectives (contributions)*: 1) The paper presents a class of parameterized, smooth, and nonlinear dynamic output feedback controllers for different domains of robotic locomotion; 2) The exponential stabilization problem under dynamic output feedback control is addressed; 3) The properties of the multi-domain Poincaré map are investigated to extend the nonlinear separation principle for the stabilization problem of hybrid periodic orbits; 4) The state feedback and observer

design problems are separately solved through the application of an offline algorithm based on an iterative sequence of BMI optimization problems; 5) Sufficient conditions are presented to guarantee the convergence of the BMI algorithm to a set of stabilizing controller and observer parameters at a finite number of iterations; 6) The power of the analytical framework is demonstrated through designing a set of HZDbased controllers integrated with an observer for dynamic walking of a 3D humanoid model with 18 state variables, 3 degrees of underactuation, 54 state feedback parameters, and 271 observer parameters; 7) The yaw stability under dynamic output feedback control is addressed; and 8) The exponential stability and robustness of the underactuated gait against external disturbances are finally illustrated through numerical simulations. Some parts of the nonlinear separation principle together with the BMI algorithm for singledomain hybrid systems were already presented in a conference paper [66] without dealing with the convergence analysis and proof, yaw stability, and robustness of the closedloop system. The current paper extends the Poincaré sections analysis, dynamic output feedback control design problem, and separation principle to multi-domain hybrid systems. It further presents more mathematical details and adds sufficient conditions to guarantee the convergence of the algorithm. The yaw stability and robustness of the closed-loop system against external disturbances are also investigated. Unlike the sufficient conditions in [33] that require extensive computational techniques based on higher-order derivatives of the Poincaré map, the new conditions only depend on the first- and second-order derivatives of the Poincaré map and thereby can be effectively and numerically verified. Existing approaches that address the separation principle for nonlinear dynamical systems are tailored to the stabilization of equilibrium points, but not multi-domain hybrid periodic orbits. In particular, the extension to periodic orbits is *not* trivial. The current paper extends the separation principle to these hybrid periodic orbits via the Poincaré sections analysis. The other contribution of the paper is that the proposed framework can systematically synthesize observerbased output feedback controllers for underactuated legged robots. In particular, unlike state-of-the-art computed torque control or augmented PD control actions that work for fullyactuated and flat-footed gaits, the proposed approach can address underactuated and dynamic gaits. Furthermore, by design, the proposed controllers can be effectively synthesized via available software packages, making the algorithms easily transferable to other robots.

2 Multi-Domain Hybrid Systems

We consider multi-domain hybrid models of legged locomotion as follows:

$$\mathscr{HL}^{\text{ol}} = (\Lambda, X, \mathcal{U}, \mathcal{D}, \mathcal{S}, \Delta, FGH),$$
 (1)

in which $\Lambda := (\mathcal{V}, \mathcal{E})$ denotes a *directed cycle* with the *vertices set* \mathcal{V} and the *edges set* $\mathcal{E} \subseteq \mathcal{V} \times \mathcal{V}$. The vertices stand

for the continuous-time dynamics of locomotion, referred to as domains or phases. The evolution of the system during each domain is expressed by ordinary differential equations (ODEs) stemming from the Lagrangian dynamics. The edges represent the discrete-time transitions between two continuous-time domains arising from the change in physical constraints (e.g., a new contact point is added to the exiting set of contact points). The evolution of the mechanical system during discrete-time transitions is assumed to be instantaneous. In this paper, we suppose that $\mu: \mathcal{V} \to \mathcal{V}$ describes the index of the next domain function for the studied locomotion pattern. Using this notation, the set of edges can be precisely described as $\mathcal{E} := \{e = (v \to \mu(v)) | v \in \mathcal{V}\}$. The set of state manifolds for (1) is represented by $X := \{X_v\}_{v \in \mathcal{V}}$ with $X_{\nu} \subseteq \mathbb{R}^n$ for some positive integer n. The set of admissible controls is denoted by $\mathcal{U} := \{\mathcal{U}_v\}_{v \in \mathcal{V}}$ with $\mathcal{U}_v \subseteq \mathbb{R}^m$ for some positive integer m < n. $\mathcal{D} := \{\mathcal{D}_v\}_{v \in \mathcal{V}}$ represents the set of domains of admissibility as a family of smooth manifolds $\mathcal{D}_v \subseteq \mathcal{X}_v \times \mathcal{U}_v$. $FGH := \{(f_v, g_v, h_v)\}_{v \in \mathcal{V}}$ then denotes the set of control systems, in which (f_v, g_v, h_v) is a control system on \mathcal{D}_{v} . In particular, the evolution of the continuoustime domain $v \in \mathcal{V}$ is expressed by the following equations:

$$\dot{x} = f_{\nu}(x) + g_{\nu}(x) u$$

$$y = h_{\nu}(x), \tag{2}$$

for $(x, u) \in \mathcal{D}_v$ with f_v , h_v , and columns of the g_v matrix being smooth (i.e., \mathcal{C}^{∞}) on \mathcal{X}_{ν} . For later purposes, we remark that $y = h_v(x) \in \mathcal{Y}_v \subseteq \mathbb{R}^{\zeta}$ represents the *measurement vector* for some positive integer $\zeta < n$. The set of guards for the hybrid system (1) is then given by $S := \{S_e\}_{e \in \mathcal{F}}$ on which the discrete transitions $e = (v \rightarrow \mu(v))$ occur when the state trajectory intersects the guard $S_{\nu \to \mu(\nu)} \subset \mathcal{X}_{\nu}$. Throughout this paper, we shall assume that the guards can be expressed as $S_{v \to \mu(v)} := \{x \in \mathcal{X}_v | s_{v \to \mu(v)}(x) = 0, \sigma_{v \to \mu(v)}(x) < 0\}, \text{ where } s_{v \to \mu(v)} : \mathcal{X}_v \to \mathbb{R} \text{ is a } C^{\infty} \text{ and } switching function } \text{satisfying the}$ regularity condition $\partial s_{\nu \to \mu(\nu)}/\partial x(x) \neq 0$ for all $x \in \mathcal{S}_{\nu \to \mu(\nu)}$. Furthermore, $\sigma_{\nu \to \mu(\nu)} : \mathcal{X}_{\nu} \to \mathbb{R}$ is a \mathcal{C}^{∞} and real-valued function to specify feasible switching points as $\sigma_{v \to u(v)}(x) < 0$. For bipedal locomotion on flat ground, $s_{\nu \to \mu(\nu)}$ can represent the height of the swing leg end with respect to the ground. In particular, events happen when $s_{\nu \to \mu(\nu)}(x) = 0$. In addition, since the height of the swing leg end is zero at the beginning and end of the step, one can exclude the case for the beginning of the step by having the vertical velocity of the swing leg end being downwards. This can be expressed as $\sigma_{v \to \mu(v)}(x) < 0$. $\Delta := \{\Delta_e\}_{e \in \mathcal{E}}$ is finally a set of reset laws to describe discrete-time transitions, where $\Delta_{\nu \to \mu(\nu)}$ is a *smooth* discrete-time system represented by $x^+ = \Delta_{\nu \to \mu(\nu)}(x^-)$ for $v \in \mathcal{V}$. In our notation, $x^-(t) := \lim_{\tau \to t} x(\tau)$ and $x^+(t) := \lim_{\tau \to t} x(\tau)$ $\lim_{\tau \searrow t} x(\tau)$ denote the left and right limits of the state trajectory x(t), respectively. Section 6.1 will utilize this hybrid systems approach for modeling of an underactuated 3D bipedal walker.

Remark 1. Models of legged locomotion can be illustrated by directed graphs including directed cycles or acyclic

graphs. Directed cycles demonstrate steady-state and periodic locomotion whereas acyclic graphs illustrate transient and aperiodic locomotion (e.g., starting from point A and going towards point B and stopping there). This paper addresses stability of periodic locomotion via dynamic output feedback controllers and thereby, we model locomotion as directed cycles.

Remark 2. To simplify the presentation of the main idea, we assume that the state variables and control inputs over different domains of the hybrid system have the same dimension, i.e., $\dim X_v = n$ and $\dim U_v = m$ for all $v \in V$. It can be shown that the results of the paper can be easily extended to hybrid models for which each domain has its own dimensions for the state variables and control inputs, i.e., $\dim X_v = n_v$ and $\dim U_v = m_v$ for some positive integers n_v and m_v .

Solutions of the hybrid model (1) are constructed by piecing together the flows of the continuous-time domains such that the discrete-time transitions occur when the state trajectories cross the switching manifolds. To make this concept more precise, we parameterize the solutions by the continuous time t as well as the vertex number v and present the following definition.

Definition 1 (Solutions). $x: [0,t_f) \times \mathcal{V} \to \mathcal{X}, t_f \in \mathbb{R}_{>0} \cup \{\infty\}$ *is said to be a solution for* (1) *if there exists* $u: [0,t_f) \times \mathcal{V} \to \mathcal{U}$ *such that*

- 1. x(t,v) and u(t,v) are right continuous on $[0,t_f)$ for every $v \in \mathcal{V}$;
- 2. The left and right limits $x^-(t,v) := \lim_{\tau \nearrow t} x(\tau,v)$ and $x^+(t,v) := \lim_{\tau \searrow t} x(\tau,v)$ exist for every $t \in (0,t_f)$ and $v \in \mathcal{V}$; and
- 3. There exists a closed discrete subset $\mathcal{T} := \{t_0 < t_1 < t_2 < \cdots\} \subset [0,t_f)$, referred to as the switching times, such that (a) for every $(t,v) \in [0,t_f) \setminus \mathcal{T} \times \mathcal{V}$, x(t,v) is differentiable with respect to t, $\frac{\partial x}{\partial t}(t,v) = f_v(x(t,v)) + g_v(x(t,v))u(t,v)$, $x^-(t,v) \notin \mathcal{S}_{v \to \mu(v)}$, and (b) for $t = t_j \in \mathcal{T}$, $x^-(t_j,v) \in \mathcal{S}_{v \to \mu(v)}$, $x^+(t_j,\mu(v)) = \Delta_{v \to \mu(v)}(x^-(t_j,v))$.

Throughout this paper, we shall assume that there is a period-one orbit for the open-loop hybrid system (1) that is transversal to the guard S. We make the following assumptions.

Assumption 1 (Periodic Solution). There exist (i) a $u^*: [0,\infty) \times \mathcal{V} \to \mathcal{U}$ and (ii) a corresponding nominal solution $x^*: [0,\infty) \times \mathcal{V} \to \mathcal{X}$ to (1) as well as (iii) a fundamental period $T^* > 0$ such that $x^*(t+T^*,v) = x^*(t,v)$ and $u^*(t+T^*,v) = u^*(t,v)$ for every $(t,v) \in \mathbb{R}_{\geq 0} \times \mathcal{V}$. The corresponding periodic orbit is then defined as

$$O := \left\{ x = x^{\star}(t, v) \mid (t, v) \in [0, T^{\star}) \times \mathcal{V} \right\}. \tag{3}$$

For later purposes, the projection of O onto the state manifold X_v is denoted by O_v .

Assumption 2 (Transversality). We suppose that O_v is transversal to the switching manifold $S_{v \to \mu(v)}$ for all $v \in \mathcal{V}$. In particular,

$$\{x_{\nu}^{\star}\} := \overline{O}_{\nu} \cap \mathcal{S}_{\nu \to \mu(\nu)} \tag{4}$$

is a singleton and $\dot{s}_{v \to \mu(v)}(x_v) \neq 0$ for all $v \in \mathcal{V}$. We remark that in our notation, O_v denotes the set closure of O_v .

The objective of this paper is to systematically design nonlinear and time-invariant dynamic output feedback controllers that exponentially stabilize the *desired* orbit *O* for the closed-loop hybrid system. For this purpose, we make use of the concept of the phasing variable. The *phasing variable* represents the system's (i.e., robot's) progression through the orbit (i.e., walking cycle), replacing the role of time in *time-invariant* feedback controllers. The following assumption makes this idea more precise.

Assumption 3 (Phasing Variable). There exists a real-valued function $\tau: X \times V \to \mathbb{R}$, referred to as the phasing variable, which is (i) C^{∞} with respect to x and (ii) strictly increasing function of time along the orbit O_v for every $v \in V$.

For later purposes, one can define the desired evolution of the state variables on the orbit O in terms of the phasing variable τ rather than t as $x^*(\tau, \nu)$.

Remark 3. We remark that Assumptions 1-3 are not restrictive for models of legged robots. In particular, transversality states that the leg ends touch the ground with nonzero vertical velocity. A typical phasing variable can be taken as the angle of the virtual stance leg, where the virtual stance leg is a virtual line connecting the stance leg end to the stance hip. For normal forward and backward walking, the angle of the virtual leg with respect to the horizontal line in the sagittal plane is strictly monotonic [14].

3 Dynamic Output Feedback Controllers

In this section, we present a class of dynamic output feedback controllers to stabilize the desired orbit O for the closed-loop hybrid system. For every continuous-time domain $v \in \mathcal{V}$, we consider a *general* form of parameterized and smooth dynamic output feedback controllers with a full-order observer portion as follows:

$$\Sigma_{v}^{c}: \begin{cases} u = \Gamma_{v}\left(\hat{x}, \xi_{v}\right), & x \in \mathcal{X}_{v} \setminus \mathcal{S}_{v \to \mu(v)} \\ \dot{\hat{x}} = f_{v}\left(\hat{x}\right) + g_{v}\left(\hat{x}\right)u + L_{v}\left(\eta_{v}\right)\left(y - \hat{y}\right) \\ \dot{\hat{y}} = h_{v}\left(\hat{x}\right) \\ \dot{\hat{x}}^{+} = \Delta_{v \to \mu(v)}\left(\hat{x}^{-}\right), & x^{-} \in \mathcal{S}_{v \to \mu(v)}. \end{cases}$$
(5)

Here, the superscript "c" and the subscript "v" stand for the controller and domain v, respectively. The class of dynamic

controllers Σ_{v}^{c} is parameterized by 1) a set of *adjustable* controller parameters $\xi_{\nu} \in \Xi_{\nu} \subset \mathbb{R}^{p_c}$ as well as 2) a set of *adjustable* observer parameters $\eta_{\nu} \in \mathbb{R}^{p_o}$ for some positive integers p_c and p_o , where $\Xi_v \subset \mathbb{R}^{p_c}$ denotes the *set of admissi*ble controller parameters. The full-order observer dynamics in (5) are taken from [60], in which the observer is a multidomain hybrid system consisting of copies of the continuousand discrete-time dynamics of the original model (1) as well as measurement injections. The switching conditions for the observer dynamics are demonstrated in terms of the switching instants of the original hybrid system. More specifically, we suppose that the switching events of the multi-domain system (1) are detectable. In practice, this assumption can be achieved by employing the contact sensors attached to the leg ends in the application of legged machines. The estimates of the state vector x and measurement vector y are then denoted by \hat{x} and $\hat{y} := h_{y}(\hat{x})$, respectively. The observer gains are represented by $L_{\nu}(\eta_{\nu}) \in \mathbb{R}^{n \times \zeta}, \nu \in \mathcal{V}$ that are parameterized by the observer parameters η_{ν} . Finally, $\Gamma_{\nu}: \mathcal{X}_{\nu} \times \Xi_{\nu} \to \mathcal{U}_{\nu}$ denotes the smooth state feedback laws parameterized by the controller parameters ξ_{ν} .

Assumption 4 (Invariant Periodic Orbit). The periodic orbit O for the closed-loop hybrid system is invariant under the choice of the controller parameters ξ , i.e.,

$$\Gamma_{\nu}(x^{\star}(t,\nu),\xi_{\nu}) = u^{\star}(t,\nu), \quad \forall (t,\nu,\xi_{\nu}) \in [0,T^{\star}) \times \mathcal{V} \times \Xi_{\nu}.$$

Example 1 (I-O Linearizing Controllers). This example presents a family of state feedback laws that satisfy the invariance condition. For a given periodic orbit O, we consider a set of controlled functions that is supposed to be regulated. Then, we design nonlinear controllers that asymptotically derive the controlled functions to zero. This can be considered as an input-output linearization (I-O) problem. Our previous work [25] shows that the stability of the periodic gaits in the I-O linearization approach depends on the proper selection of the output functions. For this reason, we consider a family of parameterized outputs that are zero on the desired orbit. We will then look for the stabilizing parameters in the controller synthesis step. More precisely, let us consider the following family of parameterized controlled functions to be regulated

$$z_{v}(x,\xi_{v}) := H_{v}(\xi_{v})(x - x^{\star}(\tau,v)),$$
 (6)

where $z_v \in \mathbb{R}^m$ represents the controlled functions with the property $dim(z_v) = dim(u) = m$. $H_v(\xi_v) \in \mathbb{R}^{m \times n}$ that is parameterized by ξ_v denotes the controlled matrix to be determined. We remark that on the orbit O, z_v is identically zero according to the construction procedure. To design the controller, suppose further that for every $\xi_v \in \Xi_v$, $z_v(x, \xi_v)$ has uniform relative degree r with respect to u on an open neighborhood of O_v , shown by $\mathcal{N}(O_v)$. The partial feedback lin-

$$\Gamma_{\nu}(x,\xi_{\nu}) = -\left(L_{g_{\nu}}L_{f_{\nu}}^{r-1}z_{\nu}\right)^{-1}\left(L_{f_{\nu}}^{r}z_{\nu} + \sum_{j=0}^{r-1}k_{j}L_{f_{\nu}}^{j}z_{\nu}\right), \quad (7)$$

where the constants k_j , $0 \le j \le r-1$ are selected such that the polynomial $\lambda^r + k_{r-1}\lambda^{r-1} + \cdots + k_1\lambda + k_0$ becomes Hurwitz. In our notation, $L_{g_v}(\cdot)$ and $L_{f_v}(\cdot)$ denote the Lie derivatives with respect to g_v and f_v , respectively. We remark that $L_{g_v}L_{f_v}^{r-1}z_v$ is an $m \times m$ square decoupling matrix that is assumed to be invertible on the periodic orbit according to the uniform relative degree r assumption. By employing (7), the output dynamics become

$$\frac{d^{r}}{dt^{r}}z_{\nu} + k_{r-1}\frac{d^{r-1}}{dt^{r-1}}z_{\nu} + \dots + k_{1}\frac{d}{dt}z_{\nu} + k_{0}z_{\nu} = 0$$
 (8)

which results in $\lim_{t\to\infty} z_{\nu}(t) = 0$. Reference [25, Example 2] shows that the feedback law (7), confined to O_{ν} , is invariant under the choice of ξ_{ν} which satisfies Assumption 4.

4 Stabilization Problem for Multi-Domain Orbits

This section addresses the exponential stabilization problem of the periodic orbit *O* under dynamic output feedback control. For this goal, we make use of the Poincaré section analysis and extend the nonlinear separation principle to the stabilization of multi-domain hybrid periodic orbits. The state feedback and observer portions will be separately synthesized in Section 5 through the application of the BMI algorithm.

4.1 Multi-Domain Closed-Loop Hybrid System

Let us define the *estimation error* and *augmented state* vector as $e := x - \hat{x} \in \mathbb{R}^n$ and $x_a := \operatorname{col}(x, e)$, respectively.

Remark 4. We remark that one can define an alternative augmented vector as $x_a := col(x, \hat{x})$. However, our choice of augmented state variables would explicitly show the separation principle in Theorem 1. In particular, the choice $x_a := col(x, e)$ would result in an upper triangular structure for the Jacobian linearization of the Poincaré map.

The evolution of the closed-loop system can then be described by the following multi-domain hybrid system

$$\mathscr{H}\mathscr{L}^{cl} = (\Lambda, \chi_a, \mathcal{S}_a, \Delta_a, F_a), \tag{9}$$

where $X_a := \{X_{a,v} := X_v \times \mathbb{R}^n\}_{v \in \mathcal{V}}$ and $S_a := \{S_{a,e} := S_e \times \mathbb{R}^n\}_{e \in \mathcal{E}}$ denote the set of augmented state manifolds and set of augmented guards, respectively. $F_a := \{f_{a,v}^{\text{cl}} := \text{col}(f_v^{\text{cl}}, \omega_v)\}$ represents the set of augmented continuous-time dynamics, i.e.,

$$\dot{x}_{a} = \begin{bmatrix} \dot{x} \\ \dot{e} \end{bmatrix} = \begin{bmatrix} f_{\nu}^{\text{cl}}(x, e, \xi_{\nu}) \\ \omega_{\nu}(x, e, \xi_{\nu}, \eta_{\nu}) \end{bmatrix} =: f_{a, \nu}^{\text{cl}}(x_{a}, \xi_{\nu}, \eta_{\nu}),$$

where

$$\begin{split} f_{\nu}^{\text{cl}}\left(x,e,\xi_{\nu}\right) &:= f_{\nu}\left(x\right) + g_{\nu}\left(x\right) \Gamma_{\nu}\left(x-e,\xi_{\nu}\right) \\ \omega_{\nu}\left(x,e,\xi_{\nu},\eta_{\nu}\right) &:= f_{\nu}\left(x\right) - f_{\nu}\left(x-e\right) \\ &+ g_{\nu}\left(x\right) \Gamma_{\nu}\left(x-e,\xi_{\nu}\right) \\ &- g_{\nu}\left(x-e\right) \Gamma_{\nu}\left(x-e,\xi_{\nu}\right) \\ &- L_{\nu}\left(\eta_{\nu}\right) \left(h_{\nu}\left(x\right) - h_{\nu}\left(x-e\right)\right). \end{split} \tag{10}$$

Finally, $\Delta_a := \{\Delta_{a,e} := \operatorname{col}(\Delta_e, \Omega_e)\}_{e \in \mathcal{E}}$ denotes the set of augmented discrete-time dynamics, i.e.,

$$x_{a}^{+} = \begin{bmatrix} x^{+} \\ e^{+} \end{bmatrix} = \begin{bmatrix} \Delta_{v \to \mu(v)} \left(x^{-} \right) \\ \Omega_{v \to \mu(v)} \left(x^{-}, e^{-} \right) \end{bmatrix} =: \Delta_{a, v \to \mu(v)} \left(x_{a}^{-} \right),$$

in which $\Omega_{\nu\to\mu(\nu)}(x,e):=\Delta_{\nu\to\mu(\nu)}(x)-\Delta_{\nu\to\mu(\nu)}(x-e)$. For later purposes, the unique solution of the smooth closed-loop ODE $\dot{x}_a=f_{a,\nu}^{\rm cl}(x_a,\xi_\nu,\eta_\nu)$ with the initial condition $x_a(0):={\rm col}(x(0),e(0))\in\mathcal{X}_{a,\nu}$ is denoted by

$$\varphi_{a,\nu}(t,x_a(0),\xi_{\nu},\eta_{\nu}) := \begin{bmatrix} \varphi_{x,\nu}(t,x_a(0),\xi_{\nu},\eta_{\nu}) \\ \varphi_{e,\nu}(t,x_a(0),\xi_{\nu},\eta_{\nu}) \end{bmatrix}$$

for all $t \geq 0$ in the maximal interval of existence, where the subscripts "x" and "e" represent the x- and e-components of the state solution, respectively. The *time-to-switching* function $T_v: \mathcal{X}_{a,v} \times \Xi_v \times \mathbb{R}^{p_o} \to \mathbb{R}_{>0}$ is then defined by $T_v(x_a(0), \xi_v, \eta_v) := \inf\{t > 0 \mid \varphi_{a,v}(t, x_a(0), \xi_v, \eta_v) \in \mathcal{S}_{a,v \to \mu(v)}\}$ as the first time at which the state trajectory $\varphi_a(t, x_a(0), \xi_v, \eta_v)$ intersects the guard $\mathcal{S}_{a,v \to \mu(v)}$.

4.2 Multi-Domain Poincaré Map

In order to exponentially stabilize the multi-domain periodic orbit, we make use of the Poincaré sections analysis that describes the evolution of the closed-loop system on a manifold transversal to the orbit, called the Poincaré section, by a discrete-time system, referred to as the Poincaré return map. For this purpose, the *generalized Poincaré map* for the domain $v \in \mathcal{V}$, denoted by $P_{a,v} : \mathcal{X}_{a,\mu^{-1}(v)} \times \Xi_v \times \mathbb{R}^{p_o} \to \mathcal{S}_{v \to \mu(v)}$, is first defined as the flow of the augmented closed-loop domain $v \in \mathcal{V}$ evaluated on $\mathcal{S}_{v \to \mu(v)}$, i.e.,

$$P_{a,\nu}\left(x_{a},\xi_{\nu},\eta_{\nu}\right) := \\ \varphi_{a,\nu}\left(T_{\nu}\left(\Delta_{a,\mu^{-1}(\nu)\to\nu}\left(x_{a}\right),\xi_{\nu},\eta_{\nu}\right),\Delta_{a,\mu^{-1}(\nu)\to\nu}\left(x_{a}\right),\xi_{\nu},\eta_{\nu}\right).$$

We next define the controller and observer parameters as $\xi := \operatorname{col}\{\xi_{\nu}\}_{\nu \in \mathcal{V}} \in \Xi \subset \mathbb{R}^{Np_c}$ and $\eta := \operatorname{col}\{\eta_{\nu}\}_{\nu \in \mathcal{V}} \in \mathbb{R}^{Np_o}$, where $N := |\mathcal{V}|$ represents the cardinal number of \mathcal{V} , and $\Xi := \Xi_{\nu_1} \times \Xi_{\nu_2} \times \cdots \Xi_{\nu_N}$. Suppose further that

$$\rho := \{v_1, \mu(v_1), \mu^2(v_1), \cdots, \mu^{N-1}(v_1)\}$$

represents the executed sequence of the vertices for the desired locomotion pattern O, in which $\mu^k(v_1) := \mu(\mu^{k-1}(v_1))$

for $k = 1, 2, \cdots$ and $\mu^0(v_1) := v_1$. We remark that according to the periodicity of the desired gait, $\mu^N(v_1) = v_1$. The *augmented Poincaré return map* is finally taken as the composition of the generalized maps $P_{a,v}$ along the switching path ρ , i.e.,

$$P_a(x_a, \xi, \eta) := P_{a,\nu_1} \circ P_{a,\mu^{N-1}(\nu_1)} \circ \cdots \circ P_{a,\mu(\nu_1)}. \tag{12}$$

By taking the Poincaré section as S_{a,v_1} , the evolution of the system can be described by the following system:

$$x_a[k+1] = P_a(x_a[k], \xi, \eta), \quad k = 0, 1, \dots,$$
 (13)

where k represents the step number. For later purposes, we decompose P_a into the x- and e-components as follows:

$$P_a(x_a, \xi, \eta) := \begin{bmatrix} P_x(x, e, \xi, \eta) \\ P_e(x, e, \xi, \eta) \end{bmatrix}. \tag{14}$$

The following lemma investigates the properties of the augmented closed-loop hybrid system.

Lemma 1 (Properties of the Poincaré Map). Assume that Assumptions 1-4 are satisfied. Then, the augmented orbit

$$O_a := O \times \{0\}$$

:= \{(x, e) = (x^*(t, v), 0) | (t, v) \in [0, T^*) \times \mathcal{V}\}

is an invariant periodic orbit for the closed-loop system (9), for all (ξ, η) , that is transversal to the guards S_a . In particular, by defining the singletons

$$\left\{x_{a,v}^{\star}\right\} := col\left(x_{v}^{\star},0\right) := \left(\overline{\mathcal{O}_{v}} \cap \mathcal{S}_{v \to \mu(v)}\right) \times \{0\},\,$$

the generalized maps $P_{a,v}, v \in \mathcal{V}$ satisfy the following invariance condition:

$$P_{a,\nu}\left(x_{a,\mu^{-1}(\nu)}^{\star},\xi_{\nu},\eta_{\nu}\right)=x_{a,\nu}^{\star},\quad\forall\left(\xi_{\nu},\eta_{\nu}\right)\in\Xi_{\nu}\times\mathbb{R}^{p_{o}}.$$

We remark that in our notation, the superscript " \star " denotes the variables corresponding to the periodic orbit.

Proof. The proof is immediate according to the construction procedure.

One immediate consequence of Lemma 1 is the existence of *invariant fixed point* x_{a,v_1}^{\star} for $P_a(\cdot,\xi,\eta)$, i.e.,

$$P_a\left(x_{a,\nu_1}^{\star},\xi,\eta\right) = x_{a,\nu_1}^{\star}, \quad \forall (\xi,\eta) \in \Xi \times \mathbb{R}^{Np_o}. \tag{15}$$

Linearization of the discrete-time system (13) around the fixed point x_{a,v_1}^{\star} then results in

$$\delta x_a[k+1] = \frac{\partial P_a}{\partial x_a} \left(x_{a,v_1}^{\star}, \xi, \eta \right) \delta x_a[k]$$
 (16)

where $\delta x_a[k] := x_a[k] - x_{a,v_1}^{\star}$.

Problem 1 (Exponential Stability). The problem of exponential stabilization of the periodic orbit O_a consists of finding the controller and observer parameters (ξ, η) such that the Jacobian matrix $\frac{\partial P_a}{\partial x_a}(x_{a,v_1}^\star, \xi, \eta)$ becomes Hurwitz. For later purposes, we define the compact notation for the Jacobian matrix as $A(\xi, \eta) := \frac{\partial P_a}{\partial x_a}(x_{a,v_1}^\star, \xi, \eta)$.

4.3 Multi-Domain Nonlinear Separation Principle

This section addresses the separation principle for exponential stabilization of multi-domain hybrid periodic orbits. The objective is to demonstrate that the problem of designing a dynamic output feedback controller for hybrid periodic orbits can be solved by designing an optimal observer for the state variables, which feeds into an optimal nonlinear controller for the hybrid system. This reduces the dynamic output feedback control synthesis problem for the augmented system into two separate parts including controller and observer syntheses.

Theorem 1 (Nonlinear Separation). Given the multi-domain hybrid system model (1) satisfying Assumptions 1-4, the following statements are correct.

1. The Jacobian matrix $A(\xi, \eta)$ has an upper triangular structure as follows:

$$A(\xi, \eta) = \begin{bmatrix} A_{11}(\xi) & A_{12}(\xi, \eta) \\ 0 & A_{22}(\eta) \end{bmatrix}, \tag{17}$$

in which $A_{11} := \frac{\partial P_x}{\partial x}(x_{\nu_1}^{\star}, 0, \xi, \eta)$, $A_{12} := \frac{\partial P_x}{\partial e}(x_{\nu_1}^{\star}, 0, \xi, \eta)$, and $A_{22} := \frac{\partial P_e}{\partial e}(x_{\nu_1}^{\star}, 0, \xi, \eta)$. Here, $P_x(\cdot)$ and $P_e(\cdot)$ denote the state and error decomposition of the Poincaré return map as defined in (14).

2. The submatrices $A_{11}(\xi)$ and $A_{22}(\eta)$ are only functions of the controller and observer parameters, respectively.

Proof. Let us define $v_{k+1} = \mu(v_k)$ for $k = 1, 2, \cdots, N - 1$. We further assume that the augmented switching manifolds $\mathcal{S}_{a,v \to \mu(v)}$ can be expressed as $\mathcal{S}_{a,v \to \mu(v)} := \{x_a \in \mathcal{X}_a \mid s_{a,v \to \mu(v)}(x_a) = 0, \sigma_{a,v \to \mu(v)}(x_a) < 0\}$, where $s_{a,v \to \mu(v)}(x_a) := s_{v \to \mu(v)}(x)$ and $\sigma_{a,v \to \mu(v)}(x_a) := \sigma_{v \to \mu(v)}(x)$. From (12) and the chain rule, the Jacobian linearization of the augmented Poincaré map P_a at x_{a,v_1}^* can be given by

$$DP_{a}(x_{a,\nu_{1}}^{\star},\xi,\eta) = DP_{a,\nu_{1}}(x_{a,\nu_{N}}^{\star},\xi_{\nu_{1}},\eta_{\nu_{1}})$$

$$\times DP_{a,\nu_{N}}(x_{a,\nu_{N-1}}^{\star},\xi_{\nu_{N}},\eta_{\nu_{N}})$$

$$\times \cdots$$

$$\times DP_{a,\nu_{2}}(x_{a,\nu_{1}}^{\star},\xi_{\nu_{2}},\eta_{\nu_{2}}).$$
(18)

We remark that according to [62, Appendix D], the Jacobian matrix $DP_{a,\nu}(x^{\star}_{a,\mu^{-1}(\nu)}, \xi_{\nu}, \eta_{\nu})$ for every $\nu \in \mathcal{V}$ can be computed as follows

$$DP_{a,\nu}(x_{a,\mu^{-1}(\nu)}^{\star},\xi_{\nu},\eta_{\nu}) = \Pi_{a,\nu}\Phi_{a,\nu}(T_{\nu}^{\star},\xi_{\nu},\eta_{\nu})D_{a,\nu}, \quad (19)$$

in which $\Pi_{a,v}$ represents the *saltation matrix* for the augmented closed-loop system defined by

$$\Pi_{a,v} := I - \frac{f_{a,v}^{cl} \left(x_{a,v}^{\star}, \xi_{v}, \eta_{v} \right) \psi}{\psi f_{a,v}^{cl} \left(x_{a,v}^{\star}, \xi_{v}, \eta_{v} \right)} \in \mathbb{R}^{2n \times 2n}, \tag{20}$$

and $\psi:=\frac{\partial s_{a,\nu} \to \mu(\nu)}{\partial x_a}\left(x_{a,\nu}^\star\right)$ is the normal vector to the guard at the singleton. In our notation, $D_{a,\nu}$ denotes the Jacobian linearization of the augmented reset law $\Delta_{a,\mu^{-1}(\nu)\to\nu}$ at $x_{a,\mu^{-1}(\nu)}^\star$, that is,

$$D_{a,v} := \frac{\partial \Delta_{a,\mu^{-1}(v) \to v}}{\partial x_a} \left(x_{a,\mu^{-1}(v)}^{\star} \right) \in \mathbb{R}^{2n \times 2n}. \tag{21}$$

Furthermore, T_{ν}^{\star} denotes the time elapsed for the nominal orbit O_{ν} to intersect $S_{\nu \to \mu(\nu)}$. $\Phi_{a,\nu}(t, \xi_{\nu}, \eta_{\nu})$ also represents the *augmented trajectory sensitivity matrix* along O_{ν} , that is,

$$\begin{split} & \Phi_{a,v}\left(t,\xi_{v},\eta_{v}\right) \\ & := \frac{\partial \varphi_{a,v}}{\partial x_{a}(0)} \left(t,\Delta_{a,\mu^{-1}(v) \to v}\left(x_{a,\mu^{-1}(v)}^{\star}\right),\xi_{v},\eta_{v}\right) \in \mathbb{R}^{2n \times 2n} \end{split}$$

which satisfies the following linear time-varying matrix differential equation, referred to as the *variational equation* (VE),

$$\begin{split} &\Phi_{a,\nu}(t,\xi_{\nu},\eta_{\nu}) = J_{a,\nu}(t,\xi_{\nu},\eta_{\nu}) \,\Phi_{a,\nu}(t,\xi_{\nu},\eta_{\nu}) \,, \,\, 0 \leq t \leq T_{\nu}^{\star} \\ &\Phi_{a,\nu}(0,\xi_{\nu},\eta_{\nu}) = I. \end{split} \tag{22}$$

In (22), $J_{a,\nu}(t,\xi_{\nu},\eta_{\nu})$ is the Jacobian linearization of the augmented vector field $f_{a,\nu}^{\rm cl}(x_a,\xi_{\nu},\eta_{\nu})$ along the nominal orbit O_{ν} , i.e.,

$$\begin{split} J_{a,v}(t,\xi_{v},\eta_{v}) &:= \frac{\partial f_{a,v}^{\text{cl}}}{\partial x_{a}} \left(x_{a},\xi_{v},\eta_{v}\right) \Big|_{x=x^{\star}(t,v),e=0} \\ &= \begin{bmatrix} \frac{\partial f_{v}^{\text{cl}}}{\partial x} \left(x,e,\xi_{v}\right) & \frac{\partial f_{v}^{\text{cl}}}{\partial e} \left(x,e,\xi_{v}\right) \\ \frac{\partial \omega_{v}}{\partial x} \left(x,e,\xi_{v},\eta_{v}\right) & \frac{\partial \omega_{v}}{\partial e} \left(x,e,\xi_{v},\eta_{v}\right) \end{bmatrix} \Big|_{x=x^{\star}(t,v),e=0} \end{split}$$

for all $(t, \xi_{\nu}, \eta_{\nu}) \in [0, T_{\nu}^{\star}] \times \Xi_{\nu} \times \mathbb{R}^{p_{o}}$. From (11), $\frac{\partial \omega_{\nu}}{\partial x}(x, 0, \xi_{\nu}, \eta_{\nu}) \equiv 0$, and consequently, one can conclude that the Jacobian matrix $J_{a,\nu}(t, \xi_{\nu}, \eta_{\nu})$ has an upper triangular structure as follows:

$$J_{a,\nu}(t,\xi_{\nu},\eta_{\nu}) = \begin{bmatrix} J_{11,\nu}(t,\xi_{\nu}) & J_{12,\nu}(t,\xi_{\nu}) \\ 0 & J_{22,\nu}(t,\eta_{\nu}) \end{bmatrix}, \quad (23)$$

in which

$$\begin{split} J_{11,\nu}\left(t,\xi_{\nu}\right) &:= \frac{\partial f_{\nu}^{\text{cl}}}{\partial x}\left(x,e,\xi_{\nu}\right)\Big|_{x=x^{\star}\left(t,\nu\right),e=0} \\ &= \frac{\partial}{\partial x}\left(f_{\nu}(x) + g_{\nu}(x)\Gamma_{\nu}\left(x,\xi_{\nu}\right)\right)\Big|_{x=x^{\star}\left(t,\nu\right)} \\ J_{12,\nu}\left(t,\xi_{\nu}\right) &:= \frac{\partial f_{\nu}^{\text{cl}}}{\partial e}\left(x,e,\xi_{\nu}\right)\Big|_{x=x^{\star}\left(t,\nu\right),e=0} \\ &= -g_{\nu}(x)\frac{\partial \Gamma_{\nu}}{\partial x}\left(x,\xi_{\nu}\right)\Big|_{x=x^{\star}\left(t,\nu\right)} \end{split}$$

are solely functions of the controller parameters ξ_{ν} . In addition, we claim that $J_{22,\nu}$ only depends on the observer parameters η_{ν} . To make this clear, we remark that

$$J_{22,\nu}(t,\eta_{\nu}) := \frac{\partial \omega_{\nu}}{\partial e} (x, e, \xi_{\nu}, \eta_{\nu}) \Big|_{x=x^{*}(t,\nu), e=0}$$

$$= \frac{\partial f_{\nu}}{\partial x} (x) \Big|_{x=x^{*}(t,\nu)}$$

$$+ \sum_{j=1}^{m} g_{\nu,j}(x) \left(\frac{\partial \Gamma_{\nu,j}}{\partial x} (x, \xi_{\nu}) - \frac{\partial \Gamma_{\nu,j}}{\partial x} (x, \xi_{\nu}) \right) \Big|_{x=x^{*}(t,\nu)}$$

$$+ \sum_{j=1}^{m} \frac{\partial g_{\nu,j}}{\partial x} (x) \Gamma_{\nu,j} (x, \xi_{\nu}) \Big|_{x=x^{*}(t,\nu)}$$

$$- L_{\nu}(\eta_{\nu}) \frac{\partial h_{\nu}}{\partial x} (x) \Big|_{x=x^{*}(t,\nu)}$$

$$= \frac{\partial f_{\nu}}{\partial x} (x) \Big|_{x=x^{*}(t,\nu)} + \sum_{j=1}^{m} \frac{\partial g_{\nu,j}}{\partial x} (x) \Big|_{x=x^{*}(t,\nu)} u_{j}^{*}(t,\nu)$$

$$- L_{\nu}(\eta_{\nu}) \frac{\partial h_{\nu}}{\partial x} (x) \Big|_{x=x^{*}(t,\nu)}, \tag{24}$$

where we have made use of the invariance condition in the sixth line of (24) as $\Gamma_{v,j}(x^*(t,v),\xi_v) = u_j^*(t,v)$ for all $\xi_v \in \Xi_v$ and $u^*(t,v)$ is the nominal control input defined in Assumption 1. According to the triangular form of the Jacobian matrix $J_{a,v}(t,\xi_v,\eta_v)$ in (23) and the structure of the VE in (22), one can conclude that the augmented trajectory sensitivity matrix can be decomposed as follows:

$$\Phi_{a,v}(t,\xi_{v},\eta_{v}) := \begin{bmatrix} \Phi_{11,v}(t,\xi_{v}) & \Phi_{12,v}(t,\xi_{v},\eta_{v}) \\ 0 & \Phi_{22,v}(t,\eta_{v}) \end{bmatrix}.$$
(25)

In particular,

$$\frac{\mathrm{d}}{\mathrm{d}t} \begin{bmatrix} \Phi_{11,\nu} & \Phi_{12,\nu} \\ 0 & \Phi_{22,\nu} \end{bmatrix} = \begin{bmatrix} J_{11,\nu} & J_{12,\nu} \\ 0 & J_{22,\nu} \end{bmatrix} \begin{bmatrix} \Phi_{11,\nu} & \Phi_{12,\nu} \\ 0 & \Phi_{22,\nu} \end{bmatrix}$$
(26)

and hence, the submatrices $\Phi_{11,\nu} \in \mathbb{R}^{n \times n}$, $\Phi_{12,\nu} \in \mathbb{R}^{n \times n}$, and $\Phi_{22,\nu} \in \mathbb{R}^{n \times n}$ satisfy the following matrix differential equa-

tions

$$\dot{\Phi}_{11,\nu}(t,\xi_{\nu}) = J_{11,\nu}(t,\xi_{\nu})\,\Phi_{11,\nu}(t,\xi_{\nu}) \tag{27}$$

$$\dot{\Phi}_{22,\nu}(t,\eta_{\nu}) = J_{22,\nu}(t,\eta_{\nu}) \,\Phi_{22,\nu}(t,\eta_{\nu}) \tag{28}$$

$$\Phi_{12,\nu}(t,\xi_{\nu},\eta_{\nu}) = J_{11,\nu}(t,\xi_{\nu}) \Phi_{12,\nu}(t,\xi_{\nu},\eta_{\nu})
+ J_{12,\nu}(t,\xi_{\nu}) \Phi_{22,\nu}(t,\eta_{\nu})$$
(29)

with the initial conditions $\Phi_{11}(0,\xi_{\nu})=I$, $\Phi_{22}(0,\eta_{\nu})=I$, and $\Phi_{12}(0,\xi_{\nu},\eta_{\nu})=0$. From the construction procedure, we can show that the saltation matrix $\Pi_{a,\nu}$ and the reset map Jacobian $D_{a,\nu}$ take block diagonal forms as follows:

$$\Pi_{a,v} = \text{block diag} \{ \Pi_{11,v}, I \}$$
 $D_{a,v} = \text{block diag} \{ D_{11,v}, D_{11,v} \},$
(30)

in which

$$\begin{split} \Pi_{11,v} := I - \frac{f_{v}^{\text{cl}}\left(x_{v}^{\star}, 0, \xi_{v}\right) \frac{\partial s_{v \to \mu(v)}}{\partial x}\left(x_{v}^{\star}\right)}{\frac{\partial s_{v \to \mu(v)}}{\partial x}\left(x_{v}^{\star}\right) f_{v}^{\text{cl}}\left(x_{v}^{\star}, 0, \xi_{v}\right)} \\ D_{11,v} := \frac{\partial \Delta_{\mu^{-1}(v) \to v}}{\partial x}\left(x_{\mu^{-1}(v) \to v}^{\star}\right). \end{split}$$

Furthermore from the invariance condition in Assumption 4, $\Pi_{11,\nu}$ and $D_{11,\nu}$ are *independent* of the choice of the controller and observer parameters (ξ_{ν}, η_{ν}) . Substituting (30) and (25) into (19) then results in

$$A_{\nu}(\xi_{\nu}, \eta_{\nu}) := DP_{a,\nu}(x_{a,\mu^{-1}(\nu)}^{\star}, \xi_{\nu}, \eta_{\nu})$$

$$= \begin{bmatrix} A_{11,\nu}(\xi_{\nu}) & A_{12,\nu}(\xi_{\nu}, \eta_{\nu}) \\ 0 & A_{22,\nu}(\eta_{\nu}) \end{bmatrix}, \quad (31)$$

for which

$$A_{11,\nu}(\xi_{\nu}) = \Pi_{11,\nu} \Phi_{11,\nu}(T_{\nu}^{\star}, \xi_{\nu}) D_{11,\nu}$$
 (32)

$$A_{12,\nu}(\xi_{\nu},\eta_{\nu}) = \Pi_{11,\nu} \Phi_{12,\nu} (T_{\nu}^{\star}, \xi_{\nu}, \eta_{\nu}) D_{11,\nu}$$
 (33)

$$A_{22,\nu}(\eta_{\nu}) = \Phi_{22,\nu}(T_{\nu}^{\star}, \eta_{\nu}) D_{11,\nu}. \tag{34}$$

Equation (31) together with (i) the chain rule in (18) and (ii) the fact that the product of upper triangular matrices is an upper triangular matrix completes the proof.

Remark 5. Although the proof of the separation principle for multi-domain periodic orbits is established based on the Poincaré map Jacobian linearization, it addresses the stabilization of these orbits for nonlinear hybrid dynamical systems. In particular, the dynamic output feedback control synthesis for the nonlinear hybrid systems can be reduced into the synthesis problems of the nonlinear state feedback laws and observers.

Remark 6. Theorem 1 illustrates the nonlinear separation principle for multi-domain hybrid periodic orbits. In particular, $eig(A(\xi,\eta)) = eig(A_{11}(\xi)) \cup eig(A_{22}(\eta))$. Therefore, O_a is exponentially stable for the augmented hybrid system, if and only if, $|eig(A_{11}(\xi))| < 1$ and $|eig(A_{22}(\eta))| < 1$.

5 BMI Algorithm for the Stabilization Problem

The objective of this section is to solve the state feedback and observer design problems through the application of an iterative algorithm based on a sequence of optimization problems involving BMIs. We also address the finite-time convergence of the algorithm to a set of stabilizing solutions.

5.1 Iterative BMI Algorithm

In order to solve for the controller and observer parameters satisfying Problem 1, we separately employ an iterative algorithm based on BMI optimizations for the state feedback and observer design problems. The BMI algorithm was developed in [25, 33] to systematically design centralized as well as decentralized nonlinear control algorithms for bipedal locomotion. Here, we employ the algorithm to design nonlinear dynamic output feedback controllers for multi-domain hybrid models of legged locomotion. The algorithm generates a sequence of controller and observer parameters, shown by $\{\xi^{\ell}\}$ and $\{\eta^{\ell}\}$, that would eventually solve Problem 1. In our notation, $\ell \in \{0, 1, 2, \dots\}$ represents the iteration number. In what follows, we briefly present the steps of the iterative algorithm adapted for the observer and state feedback synthesis. Section 5.2 will present sufficient conditions for the convergence of the algorithm to a stabilizing set of parameters at a finite number of iterations.

Step 1 (Sensitivity Analysis): During iteration ℓ of the algorithm, the Jacobian matrix $A_{22}(\eta^\ell + \Delta \eta)$ (resp., $A_{11}(\xi^\ell + \Delta \xi)$) is replaced by its first-order approximation, based on the Taylor series expansion, which is affine in $\Delta \eta$ (resp., $\Delta \xi$). Here, $\Delta \eta$ (resp., $\Delta \xi$) is a sufficiently small increment in the observer (resp., controller) parameters and the approximate Jacobian matrix is shown by $\hat{A}_{22}(\eta^\ell, \Delta \eta)$ (resp., $\hat{A}_{11}(\xi^\ell, \Delta \xi)$). In particular,

$$A_{22}\left(\eta^{\ell} + \Delta\eta\right) \approx A_{22}\left(\eta^{\ell}\right) + \bar{A}_{22}\left(\eta^{\ell}\right) (I \otimes \Delta\eta)$$

$$=: \hat{A}_{22}\left(\eta^{\ell}, \Delta\eta\right) \qquad (35)$$

$$A_{11}\left(\xi^{\ell} + \Delta\xi\right) \approx A_{11}\left(\xi^{\ell}\right) + \bar{A}_{11}\left(\xi^{\ell}\right) (I \otimes \Delta\xi)$$

$$=: \hat{A}_{11}\left(\xi^{\ell}, \Delta\xi\right), \qquad (36)$$

where " \otimes " represents the Kronecker product. \bar{A}_{11} and \bar{A}_{22} are called *sensitivity matrices* that can be computed effectively using the numerical approach of [25, Theorem 2].

Step 2 (BMI Optimization): In this step, we look for the increment $\Delta\eta$ (resp. $\Delta\xi$) such that the approximate Jacobian matrix $\hat{A}_{22}(\eta^{\ell},\Delta\eta)$ (resp. $\hat{A}_{11}(\xi^{\ell},\Delta\xi)$) becomes Hurwitz. For this purpose, we set up a BMI condition in terms of $\Delta\eta$ (resp. $\Delta\xi$) which can be solved with available software packages such as PENBMI [67]. In particular, we solve the

following BMI problem for the observer synthesis:

$$\min_{(\Delta \eta, W_2, \gamma_2, \delta)} - w \gamma_2 + \delta \tag{37}$$

s.t.
$$\begin{bmatrix} W_2 \hat{A}_{22}(\eta^{\ell}, \Delta \eta) W_2 \\ \star (1 - \gamma_2) W_2 \end{bmatrix} > 0$$
 (38)

$$\begin{bmatrix} I & \Delta \eta \\ \star & \delta \end{bmatrix} > 0 \tag{39}$$

$$\gamma_2 > 0. \tag{40}$$

Inequality (38) represents a BMI in terms of $\Delta \eta$ and W_2 to guarantee that \hat{A}_{22} is a Hurwitz matrix. In particular from the Schur complement lemma, $V(\delta x) = \delta x^{\top} W_2^{-1} \delta x$ is a Lyapunov candidate function for $\delta x[k+1] = \hat{A}_{22} \bar{\delta}x[k]$ such that $V[k+1] - V[k] < -\gamma_2 V[k]$, in which $0 < \gamma_2 < 1$ is a scalar to tune the convergence rate. Here, "**" denotes the transpose of the block (1,2). From the Schur complement lemma and LMI (39), δ is an upper bound on the 2-norm of $\Delta \eta$, i.e., $\delta > \|\Delta \eta\|_2^2$. In addition, w > 0 is a weighting factor as a trade-off between improving the convergence rate (i.e., minimizing $(1 - \gamma_2)$) and minimizing $\|\Delta \eta\|_2^2$ to have a good firstorder approximation. The motivation for the optimization problem (37)-(40) is to look for the increment in the observer parameters $\Delta \eta$ such that the approximated Jacobian matrix $\hat{A}_{22}(\eta^{\ell}, \Delta \eta)$ has all eigenvalues inside the unit circle to ensure exponential stability. In addition, it tries to minimize the 2-norm of the increment $\Delta \eta$ such that $\hat{A}_{22}(\eta^{\ell}, \Delta \eta)$ becomes a good approximation for the real Jacobian matrix. We remark that by minimizing $(1 - \gamma_2)$, the eigenvalues of the approximate Jacobian matrix get closer to the origin. In addition, by minimizing δ , the 2-norm of $\Delta \eta$ becomes smaller. For higher values of the weighting factor w in the cost function (37), we are interested more in convergence while for lower values of w, we would like to get smaller increments $\Delta \eta$. An analogous BMI optimization problem can be solved for the state feedback synthesis as follows:

$$\min_{(A^{\sharp}, W, \alpha, \delta)} - w \gamma_1 + \delta \tag{41}$$

s.t.
$$\begin{bmatrix} W_1 \ \hat{A}_{11}(\xi^{\ell}, \Delta \xi) W_1 \\ \star (1 - \gamma_1) W_1 \end{bmatrix} > 0$$
 (42)

$$\begin{bmatrix} I & \Delta \xi \\ \star & \delta \end{bmatrix} > 0 \tag{43}$$

$$\gamma_1 > 0. \tag{44}$$

Step 3 (Iteration): Let us assume that $(\Delta \eta^{\ell \star}, W_2^{\ell \star}, \gamma_2^{\ell \star}, \delta^{\ell \star})$ (resp., $(\Delta \xi^{\ell \star}, W_1^{\ell \star}, \gamma_1^{\ell \star}, \delta^{\ell \star})$) represents a local optimal solution (not necessarily the global solution) for the BMI optimization problem (37)-(40) (resp., (41)-(44)). The local minimum solution is then used to update the observer (resp., controller) parameters as $\eta^{\ell+1} = \eta^{\ell} + \Delta \eta^{\ell \star}$ (resp., $\xi^{\ell+1} = \xi^{\ell} + \Delta \xi^{\ell \star}$)) for the next iteration. If the conditions of Remark 6 are satisfied at $\eta = \eta^{\ell+1}$ (resp., $\xi = \xi^{\ell+1}$), the algorithm is successful and stops. Otherwise, it continues by coming back to Step 1 (sensitivity analysis around $\eta^{\ell+1}$ (resp., $\xi^{\ell+1}$)). If

the BMI optimization problem in Step 2 is not feasible, the algorithm is not successful and stops.

5.2 Finite-Time Convergence of the BMI Algorithm

Our previous work in [33] presented sufficient conditions to guarantee the convergence of the iterative BMI algorithm to a stabilizing feedback solution. These conditions were derived based on higher-order derivatives of the Poincaré map that require extensive computational burden. In this section, we present alternative sufficient conditions for the convergence of the algorithm that can be effectively verified without using higher-order derivatives. We assume a convex-hull of the approximate Jacobian matrices during the previous iterations and if the current real Jacobian matrix takes values in this convex-hull, the algorithm successfully converges.

Theorem 2 (Convergence of the Algorithm). Assume that Assumptions 1-4 are satisfied. Suppose further that the BMI optimization problem (37)-(40) for the observer synthesis (resp., (41)-(44) for the state feedback synthesis) is feasible during M iterations for some positive integer M. Let $\{\eta^\ell\}_{\ell=0}^M$ (resp., $\{\xi^\ell\}_{\ell=0}^M$) denote the generated sequence of observer (resp., controller) parameters from the initial guess η^0 (resp., ξ^0), i.e., $\eta^\ell = \eta^0 + \sum_{j=0}^{\ell-1} \Delta \eta^{j\star}$, (resp., $\xi^\ell = \xi^0 + \sum_{j=0}^{\ell-1} \Delta \xi^{j\star}$) for $1 \le \ell \le M$. Define the compact notation $\hat{A}_{22}^\ell := \hat{A}_{22}(\eta^\ell, \Delta \eta^{\ell\star})$ (resp., $\hat{A}_{11}^\ell := \hat{A}_{11}(\xi^\ell, \Delta \xi^{\ell\star})$) for $0 \le \ell \le M-1$ and consider the following convex-hull of approximated Jacobian matrices:

$$\begin{aligned} \mathcal{A}_{ii} &:= Conv \left\{ \hat{A}_{ii}^{\ell} \right\}_{\ell=0}^{M-1} \\ &:= \left\{ \sum_{\ell=0}^{M-1} \alpha_{\ell} \hat{A}_{ii}^{\ell} \, \middle| \, \alpha_{\ell} \geq 0, 0 \leq \ell \leq M-1, \, \sum_{\ell=0}^{M-1} \alpha_{\ell} = 1 \right\} \end{aligned}$$

for $i \in \{1,2\}$. If $A_{22}(\eta^M) \in \mathcal{A}_{22}$ (resp., $A_{11}(\xi^M) \in \mathcal{A}_{11}$), then $\eta = \eta^M$ (resp., $\xi = \xi^M$) forms a set of stabilizing observer (resp., controller) parameters.

Proof. We present the proof for the finite-time convergence of the BMI algorithm to synthesize the observer. An analogous reasoning can be presented for the state feedback synthesis. From the feasibility of the BMI optimization problem (37)-(40), $V^{\ell}(\delta x) = \delta x^{\top} \left(W_2^{\ell \star}\right)^{-1} \delta x$ is a Lyapunov candidate for the discrete-time system $\delta x[k+1] = \hat{A}_{22}^{\ell} \delta x[k]$. Since $A_{22}\left(\eta^{M}\right) \in \mathcal{A}_{22}$, there are constants $\alpha_{\ell} \geq 0$ for $0 \leq \ell \leq M-1$ with the property $\sum_{\ell=0}^{M-1} \alpha_{\ell} = 1$ such that $A_{22}\left(\eta^{M}\right) = \sum_{\ell=0}^{M-1} \alpha_{\ell} \hat{A}_{22}^{\ell}$. From [68, Theorem 2], one can then conclude that

$$V\left(\delta x\right) := \sum_{\ell=0}^{M-1} \alpha_{\ell} V^{\ell}\left(\delta x\right) = \delta x^{\top} \left(\sum_{\ell=0}^{M-1} \alpha_{\ell} \left(W_{2}^{\ell \star}\right)^{-1}\right) \delta x$$

is Lyapunov candidate for $\delta x[k+1] = A_{22}(\eta^M)\delta x[k]$, i.e., V[k+1] - V[k] < 0. In particular, the observer parameters

during the iteration M, that is η^M , can stabilize the real Jacobian matrix $A_{22}(\eta^M)$ in the sense that $|\text{eig}(A_{22}(\eta^M))| < 1$. More specifically, the iterative algorithm converges to stabilizing observer parameters which completes the proof.

Remark 7. We remark that the conditions of Theorem 2 are not restrictive. In particular, BMIs are nonconvex and NP-hard problems [69], and hence convergence to global solutions is a real challenge. Theorem 2 only requires a feasible solution of the BMI optimization for each iteration to satisfy the BMI and LMI conditions. In fact, it does not need any global solution. More specifically, if during any iteration the real Jacobian matrix belongs to the convex hull of the approximate Jacobian matrices from the previous iterations, the algorithm successfully stops.

6 Application to 3D Bipedal Walking

The objective of this section is to numerically validate the proposed analytical framework through designing a nonlinear dynamic output feedback controller for underactuated walking of a 3D bipedal robot.

6.1 Underactuated 3D Robot

We consider an underactuated bipedal robot consisting of a rigid tree structure with a torso and two identical legs terminating at point feet. Each leg of the robot includes 3 DOFs: a 2 DOF ball hip joint with roll and pitch angles plus a 1 DOF knee joint (see Fig. 1). During the single support phase, the mechanical system has 9 DOFs with 6 actuators. To specify a minimal set of configuration variables, we rigidly attach a frame to the torso link with the z-axis being upward and the y-axis being in the direction of walking. The orientation of this frame with respect to an inertial world frame is described by the rotation matrix $R := R_z(q_z) R_v(q_v) R_x(q_x)$, in which R_z , R_v , and R_x denote the basic rotations about the z-, y-, and x-axis, respectively. Furthermore, q_z , q_y , and q_x represent the yaw, roll, and pitch angles of the torso frame. The configuration vector of the robot is then defined by

$$q := \operatorname{col}(q_z, q_y, q_x, q_{\text{RK}}, q_{\text{RHS}}, q_{\text{RHF}}, q_{\text{LK}}, q_{\text{LHS}}, q_{\text{LHF}}) \in Q,$$
(45)

where $q_{\rm RK}$ and $q_{\rm LK}$ denote the right and left knee angles, $q_{\rm RHS}$ and $q_{\rm LHS}$ represent the right and left hip angles in the sagittal plane, and $q_{\rm RHF}$ and $q_{\rm LHF}$ denote the right and left hip angles in the frontal plane. The configuration space Q is also assumed to be an open and connected subset of the torus $\mathbb{T}^9 := \mathbb{S}^1 \times \cdots \times \mathbb{S}^1 \subset \mathbb{R}^9$, where $\mathbb{S}^1 := [-\pi, \pi)$ represents the unit circle. The state vector and state manifold are taken as $x := \operatorname{col}(q, \dot{q})$ and $\mathcal{X} := \operatorname{T} Q$, respectively. The control input vector u finally consists of the corresponding torques applied at the internal joints, i.e.,

$$u := \operatorname{col}(u_{RK}, u_{RHS}, u_{RHF}, u_{LK}, u_{LHS}, u_{LHF}) \in \mathcal{U} \subset \mathbb{R}^6$$
. (46)

The hybrid model of walking includes two continuoustime domains to represent the right and left stance phases

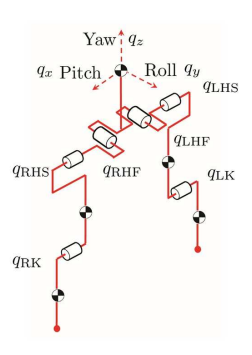


Fig. 1. Structure of the nine-DOFs autonomous bipedal robot. The model consists of a tree structure with torso and two identical legs with three unactuated Euler angles and six actuated revolute joints.

and two discrete-time transitions to represent the right-toleft and left-to-right impact models. In particular, for the open-loop hybrid model of walking (1), we have $\mathcal{V} := \{R, L\}$ and $\mathcal{E} := \{R \to L, L \to R\}$, in which the subscripts "R", "L", "R \rightarrow L", "L \rightarrow R" denote the right stance phase, left stance phase, right-to-left impact, and left-to-right impact, respectively. The continuous-time domains arise from the Lagrangian and underactuated dynamics and are given by the input-affine state equations $\dot{x} = f_R(x) + g_R(x)u$ and $\dot{x} = f_{\rm L}(x) + g_{\rm L}(x)u$, whereas the discrete-time transitions $x^+ = \Delta_{R \to L}(x^-)$ and $x^+ = \Delta_{L \to R}(x^-)$ assume rigid and instantaneous contact models [7]. The right-to-left and left-toright guards are also represented by the manifolds $\mathcal{S}_{R o L}$ and $\mathcal{S}_{L\to R}$, respectively, on which the swing leg end contacts the walking surface. The domain of admissibility $\mathcal{D} \subset \mathcal{X} \times \mathcal{U}$ is chosen as the set of all points (x, u) for which the legs are above the walking surface (i.e., unilateral constraints) and ground reaction forces are feasible (i.e., they belong to the friction cone). The kinematic and dynamic parameter values for the links are taken according to those reported in [70] from a human cadaver study. Using the motion planning algorithm of [24], a periodic gait O is then designed for walking at 0.6 (m/s) with the cost of mechanical transport CMT = 0.07.

6.2 Virtual Constraint Controllers

Virtual constraints are defined as kinematic constraints for the continuous-time domains of hybrid models of walking to coordinate the links of robots within a stride [71,72, 17, 22, 73, 24, 21, 18, 30, 31, 32, 34, 35]. In this paper, we consider a parameterized family of virtual constraints for the continuous-time domain $v \in \mathcal{V}$ as follows:

$$z_{\nu}(x,\xi_{\nu}) := H_{\nu}(\xi_{\nu}) (q - q^{\star}(\tau,\nu)),$$
 (47)

where $\dim(z_v) = \dim(u) = 6$, $H_v(\xi_v) \in \mathbb{R}^{6\times 9}$ denotes the controlled matrix to be determined and parameterized by the controller parameters ξ_v , and $q^*(\tau, v)$ represents the desired evolution of the configuration variables on the orbit O_v in terms of the gait phasing variable τ . The phasing variable τ is taken as the angle of the virtual leg with respect to the horizontal line, where the *virtual leg* is defined as the virtual line

connecting the stance foot to the stance hip joint in the sagittal plane. For later purposes, we remark that $H_{\nu}(\xi_{\nu})q$ and $H_{\nu}(\xi_{\nu})q^{\star}(\tau,\nu)$ denote a set of holonomic quantities, referred to as the *controlled variables*, and the desired evolution of the controlled variables on the gait, respectively. The state feedback is then chosen as the partial feedback linearizing controller of Example 1 for which uniform relative degree r is assumed to be 2. We assume that ξ_{ν} is formed by the columns of the controlled matrix H_{ν} , that is, $\xi_{\nu} = \text{vec}(H_{\nu}) \in \Xi_{\nu} \subset \mathbb{R}^{54}$, where "vec" denotes the matrix vectorization operator.

For bipedal robots with more than one degree of underactuation, it has been shown that the stability of walking gaits depends on the choice of the virtual constraints (i.e., controlled variables) [25,74]. To exponentially stabilize the gait, we employ the iterative BMI algorithm to look for stabilizing controller parameters $\xi := \operatorname{col}(\xi_R, \xi_L)$. Since the orbit is assumed to be symmetric, one can apply the symmetric relation between ξ_R and ξ_L to reduce the number of decision variables to be determined (see [25, Theorem 4]). This procedure is followed in this paper.

6.3 PENBMI Solver for Controller Synthesis

This section addressees the synthesis and tuning of controller parameters. Here the relative degree is r = 2 and the constant gains k_i for j = 0, 1 are chosen such that the settling time for the output dynamics (8) becomes 20 (ms). We then look for the output matrices $H_{\nu}(\xi_{\nu})$ via the iterative BMI algorithm. To solve the BMI optimization problem at each iteration of the algorithm, we make use of the PENBMI solver from TOMLAB [75] integrated with the MATLAB environment through YALMIP [76]. BMIs are nonconvex and NPhard problems [69]. However, PENBMI is a general-purpose solver for BMIs, which guarantees the convergence to a local optimal point satisfying the Karush-Kuhn-Tucker optimality conditions. The BMI algorithm for the state feedback synthesis starts with an initial set of controller parameters ξ^0 for which $H(\xi^0)q$ represents the actuated shape variables. For this set of controller parameters, the dominant eigenvalues and spectral radius of the 17×17 Jacobian matrix A_{11} become $\{-4.0307, -1.000, 0.7915, -0.262\}$ and 4.0307, respectively, and hence, the gait is unstable. After four iterations, the algorithm successfully converges to a stabilizing set of controller parameters for which the dominant 0.7446i, 0.5309, -0.4176 and 0.7621, respectively.

6.4 Observer Synthesis

In this subsection, a future application in prosthetic/exoskeleton control is studied. In particular, we would like to investigate if one can asymptotically estimate all state variables for mechanical models of human locomotion (see Fig. 1) while there is a set of wearable inertial measurement units (IMUs) that measure absolute position variables. More specifically, we suppose that there are five IMUs connected to the torso, right and left femurs, and right and left tibias of the system depicted in Fig. 1. The measurements then include the five roll, pitch, and yaw signals, i.e.,

 $y = h_{\nu}(x) \in \mathbb{R}^{15}, \nu \in \mathcal{V}$. Let us express the position measurements from the network of IMUs by $\bar{q} := h_{\nu}(x) \in \mathbb{R}^{15}$. We can show that the minimal set of configuration variables is related to \bar{q} as follows:

$$q = F(\bar{q}), \tag{48}$$

where $F:\mathbb{T}^{15}\to\mathbb{T}^9$ is a nonlinear function arising from inverse kinematics. We remark that in general there is *not* a closed-form expression for F which complicates the use of optimal state feedback laws in terms of (q,\dot{q}) . To overcome this difficulty, we instead design a full-order observer to estimate (q,\dot{q}) using \bar{q} measurements. Unlike the high-gain observer of [60], the proposed optimized observer can asymptotically solve for (48), and accordingly, there is *no* need to design an alternative state feedback in terms of the nonminimal coordinates $(\bar{q},\dot{\bar{q}})$ for the stabilization of walking gaits.

Remark 8. We remark that IMUs can provide both absolute orientations and angular velocities. Let us denote the absolute position and angular velocities generated by IMUs by \bar{q} and $\bar{\omega}$, respectively. These variables can be related to the original state variables through the following nonlinear equations

$$q = F(\bar{q}) \tag{49}$$

$$\bar{\omega} = J_{\omega}(q)\dot{q},$$

where $J_{\omega}(q)$ is an associated Jacobian matrix. Our problem consists of estimating the state variables $x = col(q,\dot{q})$ based on IMU measurements as the state feedback controllers are expressed in terms of the state variables. Since in general, there is not any closed-from expression for $F(\cdot)$ from the inverse kinematics, one cannot easily solve for q and \dot{q} for high degree of freedom 3D models of legged robots. However, the proposed observer can asymptotically estimate q and \dot{q} without any need for inverse kinematics and only by measuring \bar{q} . In the current paper, we do not use the angular velocity signals $\bar{\omega}$ for the observer synthesis to illustrate the power of the proposed approach. But one can easily utilize these additional inputs for the observer synthesis.

The observer gains are assumed to take the following form:

$$L_{\nu} := \frac{1}{\varepsilon} L_{0,\nu} \in \mathbb{R}^{18 \times 15},$$
 (50)

in which $0 < \varepsilon < 1$ is a sufficiently small number. The columns of $L_{0,\nu}$ together with ε form the observer parameters, that is, $\eta_{\nu} := \operatorname{col}(\operatorname{vec}(L_{0,\nu}), \varepsilon) \in \mathbb{R}^{271}$. We remark that the inclusion of ε in decision variables would let the BMI algorithm search for high-gain observers if required. Here, we follow an approach similar to the symmetry analysis in [25, Theorem 4] to reduce the number of parameters to be determined. We start the BMI algorithm with an initial

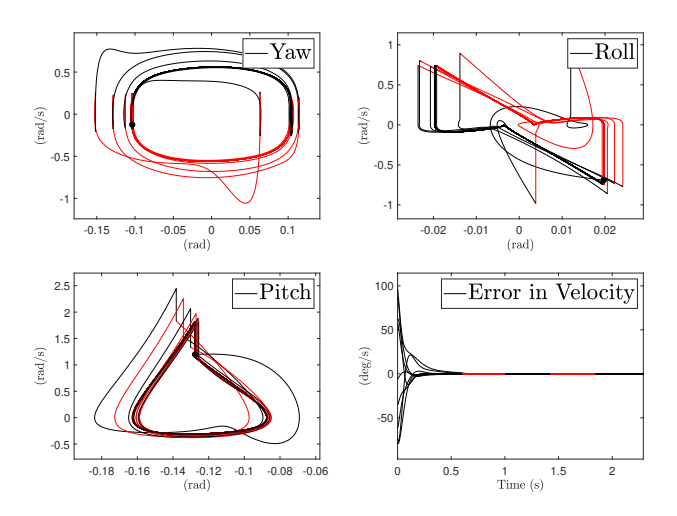


Fig. 2. Phase portraits for the torso Euler angles (yaw, roll, and pitch) during 100 consecutive steps together with the velocity estimation error during 5 consecutive steps of 3D walking with the BMI-optimized dynamic output feedback controller.

set of observer parameters for which the 18×18 Jacobian matrix A_{22} has the dominant eigenvalues and spectral radius of $\{26.8856, 0.1129, -0.0095, 0.0079\}$ and 26.8856, respectively. The algorithm successfully converges to a set of stabilizing observer parameters after 19 iterations, for which the spectral radius of A_{22} becomes 0.0053.

The estimation error in the velocity components versus time and phase portraits for the BMI-optimized closed-loop system are illustrated in Fig. 2. Here, the simulation starts off of the orbit at the beginning of the right stance phase with an estimation error of 90% in the velocity components. Asymptotic convergence to the periodic orbit even in the yaw component (i.e., full-state stability) is clear. The stabilizing controller and observer parameters computed based on the BMI algorithm together with the animation of this simulation can be found at [77]. To confirm the robustness of the walking gait against external disturbance forces, Fig. 3 represents the phase portraits and velocity estimation error for the closedloop system. Here the simulation starts at the initial condition of Fig. 2. During the fifth step, an external horizontal force with a magnitude of 70 (N) is applied to the robot's center of mass in the frontal plane for 20% of the step.

6.5 Exponential Stability Modulo Yaw

For bipedal robots with yaw motion, there are two kinds of stability during walking on a flat surface: *full-state stability* and *stability modulo yaw*. Full-state stability refers to stability in X as shown in Fig. 2. If the closed-loop hybrid system is equivariant under rotations about the z-axis of the world frame, then the Jacobian of the Poincaré map always has an eigenvalue at 1.0, and hence the closed-loop system cannot have an exponentially stable periodic orbit. Stability modulo yaw refers to stability in $X \setminus \mathbb{S}^1$ which is simpler than full-state stability. In particular, one may be interested in stabilizing the locomotion pattern but not the direction of locomotion. More specifically, stability modulo yaw relaxes the stability in the yaw component. This section aims to show

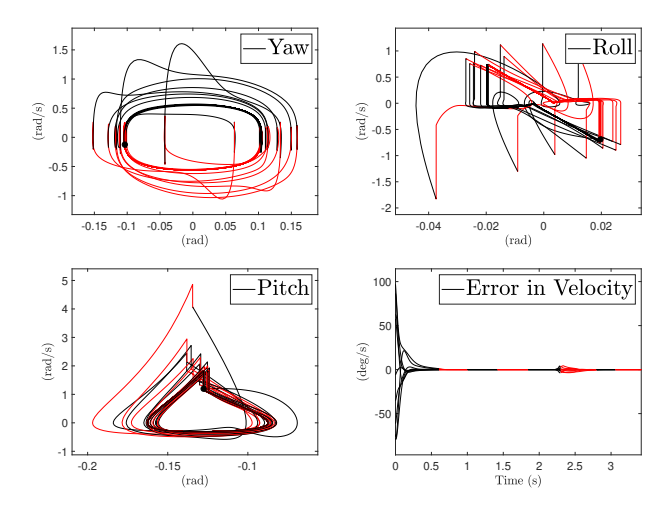


Fig. 3. Phase portraits for the torso Euler angles (yaw, roll, and pitch) and velocity estimation error for the BMI-optimized closed-loop system in the presence of an external disturbance during the fifth step. Convergence to the periodic orbit and disturbance rejection are clear.

how the proposed approach can be reduced to stability modulo yaw. References [78, 79, 80] have studied stability modulo yaw for hybrid models of walking with state feedback controllers. The objective of this section is to extend stability modulo yaw to hybrid models with dynamic output feedback controllers. In particular, we present the following result.

Proposition 1 (Stability Modulo Yaw). Consider the multi-domain hybrid model of 3D robotic locomotion with the dynamic output feedback control (5). Assume that the configuration vector q is expressed as $q := col(q_z, q_y, q_x, q_b)$, where q_z , q_y , and q_x represent the yaw, roll, and pitch angles of the robot with respect to the world frame, respectively. In addition, let q_b denote a set of body configuration variables describing the shape of the robot. Suppose further that the periodic orbit O corresponds to a walking gait on a flat surface. Then, the following statements are correct.

- 1. If the measurement vectors $h_{\nu}(x), \nu \in \mathcal{V}$ do not depend on the yaw position (i.e., $\frac{\partial h_{\nu}}{\partial q_z}(x) \equiv 0$), then the first column of the $A_{22}(\eta)$ matrix is $col(1,0,\cdots,0)$. In particular, there is an eigenvalue "1" corresponding to the yaw position.
- 2. If the state feedback laws $\Gamma_{\nu}(x,\xi_{\nu}), \nu \in \mathcal{V}$ do not depend on the yaw position (i.e., $\frac{\partial \Gamma_{\nu}}{\partial q_z}(x,\xi_{\nu}) \equiv 0$), then the first column of the $A_{11}(\eta)$ matrix is $col(1,0,\cdots,0)$. In particular, there is an eigenvalue "1" corresponding to the yaw position.

Proof. We prove Part (1) which is about the observer portion. Part (2) has been addressed in [78, 10] for state feedback controllers. From the *equivariance property* of [78], the vector field f_v and the columns of the g_v matrix do not depend on the yaw position, that is, $\frac{\partial f_v}{\partial q_z}(x) = 0$ and $\frac{\partial g_{v,j}}{\partial q_z}(x) = 0$ for $v \in \mathcal{V}, 1 \leq j \leq m$. This property also states that $\partial \Delta_{v \to \mu(v)}/\partial q_z(x) = \operatorname{col}(1,0,\cdots,0)$. If h_v is not a function of q_z , then the first column of the $J_{22,v}(t,\eta)$ matrix in

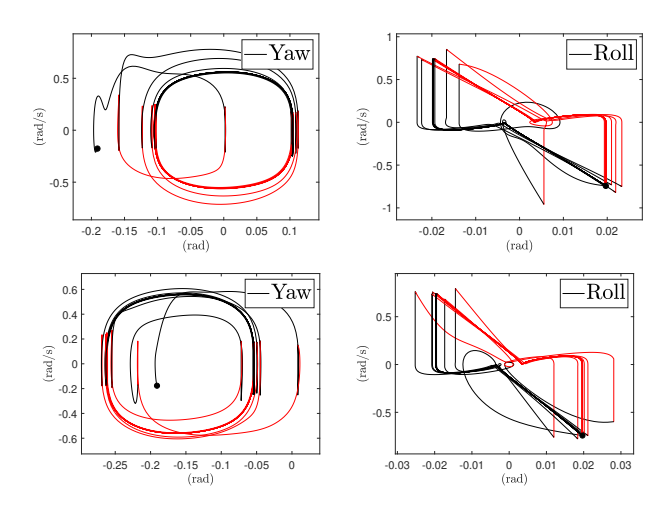


Fig. 4. Phase portraits for the torso Euler angles (yaw and roll) during 50 consecutive steps of 3D walking with the BMI-optimized output feedback controller. For the top plots, the measurement vector $h_{\nu}(x)$ includes the yaw angles from the IMUs, whereas for the bottom plots the yaw angle portions of $h_{\nu}(x)$ are assumed to be unavailable. We observer full-state stability and stability modulo yaw.

(24) becomes zero. From this latter fact and the VE (28), one can conclude that the first column of the state trajectory matrix $\Phi_{22,\nu}(t,\eta)$ is $\operatorname{col}(1,0,\cdots,0)$. Finally, substituting $\Phi_{22,\nu}(T_{\nu}^{\star},\eta)$ and $D_{11,\nu}=\partial \Delta_{\mu^{-1}(\nu)\to\nu}/\partial x(x_{\mu^{-1}(\nu)}^{\star})$ in (34) completes the proof.

Remark 9 (BMIs for Stability Modulo Yaw). If the assumptions of Proposition 1 are satisfied, one can apply the BMI algorithm to reduced-order matrices $\check{A}_{22}(\eta)$ and $\check{A}_{11}(\xi)$) to guarantee exponential stability modulo yaw, where $\check{A}_{22}(\eta)$ and $\check{A}_{11}(\xi)$ represent the submatrices obtained by removing the first row and column of $A_{22}(\eta)$ and $A_{11}(\eta)$, respectively.

To confirm the analytical result of Proposition 1, we assume that the yaw angle measurements from the network of IMUs are not available for the BMI-optimized dynamic output feedback controller. In particular, one can assume that there is a considerable amount of drift in the yaw angle measurements. In this case, from Part (1) of Proposition 1, we can still have stability modulo yaw. However, we are not able to asymptotically estimate q_z (i.e., the torso yaw angle). Figures 4 and 5 compare the phase portraits and estimation errors for full-state stability and stability modulo yaw. Here, the simulation starts off of the desired gait O. We observe that the steady-state motion in the phase plane $q_z - \dot{q}_z$ for stability modulo yaw is the shifted version of that for full-state stability. Specifically, the robot walks along a new straight line rather than the y-axis of the world frame. Furthermore, $\lim_{t\to\infty} e_1(t)$ becomes a nonzero and constant value, where e_1 represents the estimation error in q_z . Figure 6 finally depicts the simulation snapshots of the walking of the underactuated robot using the optimized dynamic output feedback controller for full-state stability and stability modulo yaw.

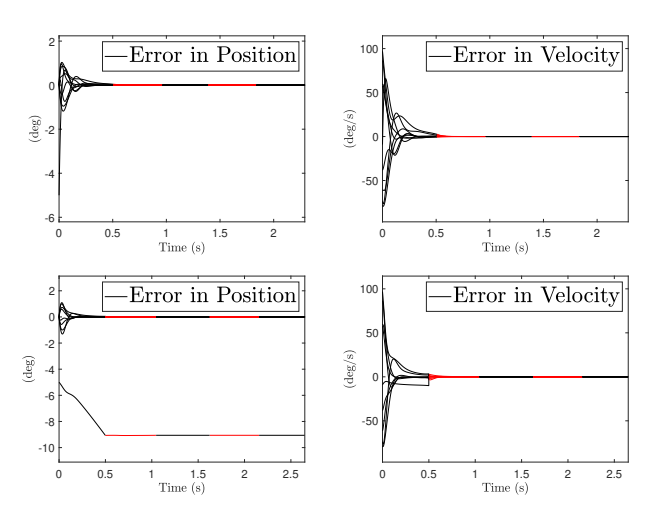


Fig. 5. Position and velocity estimation errors over 5 consecutive steps of 3D walking with the BMI-optimized output feedback controller. For the top plots, the measurement vector $h_{\nu}(x)$ includes the yaw angles from the IMUs, whereas for the bottom plots the yaw angle portions of $h_{\nu}(x)$ are assumed to be unavailable. We observer that the steady-state estimation error in the torso yaw angle is a nonzero constant, i.e., $0 \neq \lim_{t \to \infty} e_1(t) < \infty$.

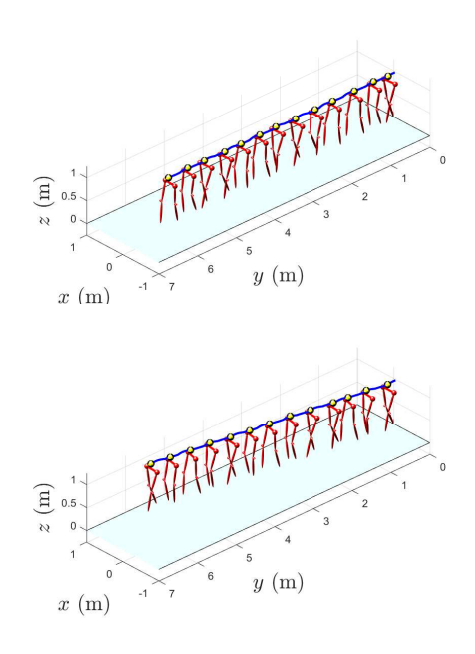


Fig. 6. Simulation snapshots from the walking of the underactuated robot using the BMI-optimized dynamic output feedback controller for full-state stability (top figure) and stability modulo yaw (bottom figure). The figures illustrate the trajectory traced by the robot's center of mass. The robot's torso link has not been shown in the figures.

6.6 Discussion

State-of-the-art nonlinear control design methods for legged robots mainly assume that all state variables are available for feedback in real time. Unfortunately, the entire state is usually too expensive to measure for legged robots with high degrees of freedom or impossible to measure for prostheses as the human users cannot be wired with a profusion of sensors. In addition, existing observer design approaches for nonlinear dynamical systems, including hybrid systems,

pertain to the estimation of state variables around equilibrium points and not periodic orbits that correspond to dynamic gaits. This paper presents a systematic framework to synthesize stabilizing nonlinear controllers for dynamic gaits of underactuated legged robots with a limited set of measurements. In particular, the extension of the separation principle to the stabilization of multi-domain hybrid period orbits in Theorem 1 together with the proposed BMI optimizationbased synthesis approach provides us a powerful computational technique to design dynamic output feedback controllers for sophisticated models of legged machines. The convergence of the algorithm has also been addressed in Theorem 2. The numerical results of the paper also illustrate the asymptotic stability of dynamic gaits for walking of an underactuated and 3D human model with 18 state variables for which the controller and observer synthesis problems can be effectively done with available software packages. The designed controllers can address external disturbances as well as asymptotic state estimation. Our previous work has experimentally shown that BMI-optimized nonlinear state feedback controllers can yield stable and dynamic walking of the bipedal robot ATRIAS on point feet [64,25] (see online [65]). We will transfer the BMI-optimized dynamic output feedback controllers into experiments in future work.

7 Conclusion

In this paper, we presented an analytical foundation to synthesize dynamic output feedback controllers for multidomain hybrid systems arising from robotic locomotion. A class of parameterized observer-based output feedback controllers was introduced for different domains of the hybrid models. The exponential stabilization problem of hybrid periodic orbits was addressed through the application of the Poincaré sections analysis. In particular, the paper extended the separation principle to the stabilization of multi-domain hybrid periodic orbits. An iterative BMI optimization algorithm was then employed to separately search for stabilizing observer and controller parameters at a finite number of iterations. Sufficient conditions for the convergence of the BMI algorithm to a set of stabilizing parameters were also presented. Furthermore, the paper addressed the fullstate stability and stability modulo yaw under dynamic output feedback controllers. To investigate the power of this analytical framework, a dynamic output feedback controller was designed for an underactuated 3D humanoid model with 18 state variables and 325 controller parameters to be determined. The numerical simulations showed the effectiveness of the approach and the robustness of the closed-loop system against external disturbances.

For future research, we will investigate the scalability and capability of the algorithm in stabilizing periodic orbits for higher-dimensional hybrid models of legged machines. To increase the robustness of dynamic walking gaits on rough terrains, we will also consider designing \mathcal{H}_2 - and \mathcal{H}_{∞} -optimal dynamic output feedback controllers [81, 82]. An alternative future direction will be optimizing the number of measurements required to have stable walking of au-

tonomous robots and amputee locomotion. Finally, as a practical application of this framework, we will use it to implement controllers for powered prosthetic legs used by lower-limb amputees.

Acknowledgments

This material is based upon work supported by the National Science Foundation under Grant Numbers 1854898 and 1906727. The content is solely the responsibility of the authors and does not necessarily represent the official views of the NSF. R. D. Gregg holds a Career Award at the Scientific Interface from the Burroughs Wellcome Fund.

References

- [1] Diop, S., Grizzle, J., Moraal, P., and Stefanopoulou, A., 1994. "Interpolation and numerical differentiation for observer design". In American Control Conference, 1994, Vol. 2, pp. 1329–1333 vol.2.
- [2] Bainov, D., and Simeonov, P., 1989. *Systems With Impulse Effect: Stability, Theory and Applications*. Ellis Horwood Ltd, June.
- [3] Ye, H., Michel, A., and Hou, L., 1998. "Stability theory for hybrid dynamical systems". *Automatic Control, IEEE Transactions on*, **43**(4), Apr, pp. 461–474.
- [4] Haddad, W., Chellaboina, V., and Nersesov, S., 2006. Impulsive and Hybrid Dynamical Systems: Stability, Dissipativity, and Control. Princeton University Press, July.
- [5] Goebel, R., Sanfelice, R., and Teel, A., 2012. *Hybrid Dynamical Systems: Modeling, Stability, and Robustness*. Princeton University Press, March.
- [6] Grizzle, J. W., Chevallereau, C., Sinnet, R. W., and Ames, A. D., 2014. "Models, feedback control, and open problems of 3D bipedal robotic walking". *Automatica*, 50(8), pp. 1955–1988.
- [7] Hurmuzlu, Y., and Marghitu, D. B., 1994. "Rigid body collisions of planar kinematic chains with multiple contact points". pp. 82–92.
- [8] Goswami, A., 1999. "Postural Stability of Biped Robots and the Foot-Rotation Indicator (FRI) Point". *The International Journal of Robotics Research*, **18**(6), pp. 523–533.
- [9] Vukobratović, M., Borovac, B., and Surla, D., 1990. *Dynamics of Biped Locomotion*. Springer.
- [10] Spong, M., and Bullo, F., 2005. "Controlled symmetries and passive walking". *Automatic Control, IEEE Transactions on*, **50**(7), July, pp. 1025–1031.
- [11] Ames, A., and Sastry, S., 2006. "Hybrid geometric reduction of hybrid systems". In Decision and Control, 45th IEEE Conference on, pp. 923–929.
- [12] Ames, A., Gregg, R., and Spong, M., 2007. "A geometric approach to three-dimensional hipped bipedal robotic walking". In Decision and Control, 46th IEEE Conference on, pp. 5123–5130.
- [13] Manchester, I., Mettin, U., Iida, F., and Tedrake, R., 2011. "Stable dynamic walking over uneven terrain".

- *The International Journal of Robotics Research*, **30**(3), pp. 265–279.
- [14] Westervelt, E., Grizzle, J., and Koditschek, D., 2003. "Hybrid zero dynamics of planar biped walkers". *Automatic Control, IEEE Transactions on*, **48**(1), Jan, pp. 42–56.
- [15] Westervelt, E., Grizzle, J., Chevallereau, C., Choi, J., and Morris, B., 2007. *Feedback Control of Dynamic Bipedal Robot Locomotion*. Taylor & Francis/CRC.
- [16] Morris, B., and Grizzle, J., 2009. "Hybrid invariant manifolds in systems with impulse effects with application to periodic locomotion in bipedal robots". *Automatic Control, IEEE Transactions on*, **54**(8), Aug, pp. 1751–1764.
- [17] Chevallereau, C., Abba, G., Aoustin, Y., Plestan, F., Westervelt, E., Canudas-de Wit, C., and Grizzle, J., 2003. "RABBIT: a testbed for advanced control theory". *Control Systems Magazine*, *IEEE*, 23(5), Oct, pp. 57–79.
- [18] Saglam, C. O., and Byl, K., 2015. "Meshing hybrid zero dynamics for rough terrain walking". In 2015 IEEE International Conference on Robotics and Automation (ICRA), pp. 5718–5725.
- [19] Sreenath, K., Park, H.-W., Poulakakis, I., and Grizzle, J. W., 2011. "Compliant hybrid zero dynamics controller for achieving stable, efficient and fast bipedal walking on MABEL". *The International Journal of Robotics Research*, 30(9), Aug., pp. 1170–1193.
- [20] Sreenath, K., Park, H.-W., Poulakakis, I., and Grizzle, J., 2013. "Embedding active force control within the compliant hybrid zero dynamics to achieve stable, fast running on MABEL". *The International Journal of Robotics Research*, 32(3), pp. 324–345.
- [21] Park, H.-W., Ramezani, A., and Grizzle, J., 2013. "A finite-state machine for accommodating unexpected large ground-height variations in bipedal robot walking". *Robotics, IEEE Transactions on*, **29**(2), April, pp. 331–345.
- [22] Martin, A. E., Post, D. C., and Schmiedeler, J. P., 2014. "The effects of foot geometric properties on the gait of planar bipeds walking under HZD-based control". *The International Journal of Robotics Research*, **33**(12), pp. 1530–1543.
- [23] Lack, J., Powell, M., and Ames, A., 2014. "Planar multi-contact bipedal walking using hybrid zero dynamics". In Robotics and Automation, IEEE International Conference on, pp. 2582–2588.
- [24] Ramezani, A., Hurst, J., Akbai Hamed, K., and Grizzle, J., 2013. "Performance analysis and feedback control of ATRIAS, a three-dimensional bipedal robot". *Jour*nal of Dynamic Systems, Measurement, and Control December, ASME, 136(2), December.
- [25] Akbari Hamed, K., Buss, B., and Grizzle, J., 2016. "Exponentially stabilizing continuous-time controllers for periodic orbits of hybrid systems: Application to bipedal locomotion with ground height variations". *The International Journal of Robotics Research*, 35(8), pp. 977–999.

- [26] Akbari Hamed, K., and Grizzle, J., 2014. "Event-based stabilization of periodic orbits for underactuated 3-D bipedal robots with left-right symmetry". *Robotics, IEEE Transactions on,* **30**(2), April, pp. 365–381.
- [27] Zhao, H., Hereid, A., Ma, W.-l., and Ames, A. D., 2015. "Multi-contact bipedal robotic locomotion". *Robotica*, pp. 1–35.
- [28] Hereid, A., Cousineau, E. A., Hubicki, C. M., and Ames, A. D., 2016. "3D dynamic walking with underactuated humanoid robots: A direct collocation framework for optimizing hybrid zero dynamics". In 2016 IEEE International Conference on Robotics and Automation (ICRA), pp. 1447–1454.
- [29] Reher, J. P., Hereid, A., Kolathaya, S., Hubicki, C. M., and Ames, A. D., 2016. "Algorithmic foundations of realizing multi-contact locomotion on the humanoid robot DURUS". In Twelfth International Workshop on Algorithmic Foundations on Robotics.
- [30] Gregg, R., Lenzi, T., Hargrove, L., and Sensinger, J., 2014. "Virtual constraint control of a powered prosthetic leg: From simulation to experiments with transfemoral amputees". *Robotics, IEEE Transactions on*, **30**(6), Dec, pp. 1455–1471.
- [31] Gregg, R., and Sensinger, J., 2014. "Towards biomimetic virtual constraint control of a powered prosthetic leg". *Control Systems Technology, IEEE Transactions on,* **22**(1), Jan, pp. 246–254.
- [32] Zhao, H., Horn, J., Reher, J., Paredes, V., and Ames, A., 2016. "Multicontact locomotion on transfemoral prostheses via hybrid system models and optimizationbased control". *IEEE Transactions on Automation Science and Engineering*, 13(2), April, pp. 502–513.
- [33] Akbari Hamed, K., and Gregg, R. D., 2017. "Decentralized feedback controllers for robust stabilization of periodic orbits of hybrid systems: Application to bipedal walking". *Control Systems Technology, IEEE Transactions on*, 25(4), July, pp. 1153–1167.
- [34] Agrawal, A., Harib, O., Hereid, A., Finet, S., Masselin, M., Praly, L., Ames, A., Sreenath, K., and Grizzle, J., 2017. "First steps towards translating HZD control of bipedal robots to decentralized control of exoskeletons". *IEEE Access*, 5, pp. 9919–9934.
- [35] Poulakakis, I., and Grizzle, J., 2009. "The spring loaded inverted pendulum as the hybrid zero dynamics of an asymmetric hopper". *Automatic Control, IEEE Transactions on*, **54**(8), Aug, pp. 1779–1793.
- [36] Akbari Hamed, K., Sadati, N., Gruver, W., and Dumont, G., 2011. "Exponential stabilisation of periodic orbits for running of a three-dimensional monopedal robot". *Control Theory Applications, IET*, 5(11), July, pp. 1304–1320.
- [37] Cao, Q., and Poulakakis, I., 2016. "Quadrupedal running with a flexible torso: control and speed transitions with sums-of-squares verification". *Artificial Life and Robotics*, **21**(4), Dec, pp. 384–392.
- [38] Isidori, A., 1995. Nonlinear Control Systems. Springer; 3rd edition.
- [39] Ciccarella, G., Mora, M. D., and Germani, A., 1993. "A

- Luenberger-like observer for nonlinear systems". *International Journal of Control*, **57**(3), pp. 537–556.
- [40] Rajamani, R., 1998. "Observers for lipschitz nonlinear systems". *IEEE Transactions on Automatic Control*, **43**(3), Mar, pp. 397–401.
- [41] Arcak, M., and Kokotovic, P., 2001. "Nonlinear observers: a circle criterion design and robustness analysis". *Automatica*, **37**(12), pp. 1923 1930.
- [42] Zemouche, A., and Boutayeb, M., 2013. "On LMI conditions to design observers for Lipschitz nonlinear systems". *Automatica*, **49**(2), pp. 585 591.
- [43] Wang, Y., and Rajamani, R., 2016. "Feasibility analysis of the bilinear matrix inequalities with an application to multi-objective nonlinear observer design". In 2016 IEEE 55th Conference on Decision and Control (CDC), pp. 3252–3257.
- [44] Goh, K., Safonov, M., and Ly, J., 1996. "Robust synthesis via bilinear matrix inequalities". *International Journal of Robust Nonlinear Control*, **6**(9-10), pp. 1079–1095
- [45] VanAntwerp, J., and Braatz, R., 2000. "A tutorial on linear and bilinear matrix inequalities". *Journal of Process Control*, **10**(4), August, pp. 363–385.
- [46] Atassi, A., and Khalil, H., 1999. "A separation principle for the stabilization of a class of nonlinear systems". *IEEE Transactions on Automatic Control*, **44**(9), Sep, pp. 1672–1687.
- [47] Ahrens, J., and Khalil, H., 2009. "High-gain observers in the presence of measurement noise: A switched-gain approach". *Automatica*, **45**(4), pp. 936 943.
- [48] Prasov, A. A., and Khalil, H. K., 2013. "A nonlinear high-gain observer for systems with measurement noise in a feedback control framework". *IEEE Transactions on Automatic Control*, **58**(3), March, pp. 569–580.
- [49] Sanfelice, R. G., and Praly, L., 2011. "On the performance of high-gain observers with gain adaptation under measurement noise". *Automatica*, **47**(10), pp. 2165 2176.
- [50] Krener, A., and Isidori, A., 1983. "Linearization by output injection and nonlinear observers". *Systems & Control Letters*, **3**(1), pp. 47 52.
- [51] Raghavan, S., and Hedrick, J., 1994. "Observer design for a class of nonlinear systems". *International Journal of Control*, **59**(2), pp. 515–528.
- [52] Gauthier, J. P., Hammouri, H., and Othman, S., 1992. "A simple observer for nonlinear systems applications to bioreactors". *IEEE Transactions on Automatic Control*, 37(6), Jun, pp. 875–880.
- [53] Teel, A., and Praly, L., 1994. "Global stabilizability and observability imply semi-global stabilizability by output feedback". *Syst. Control Lett.*, **22**(5), May, pp. 313–325.
- [54] Maggiore, M., and Passino, K. M., 2003. "A separation principle for a class of non-uco systems". *IEEE Trans*actions on Automatic Control, 48(7), July, pp. 1122– 1133.
- [55] Arcak, M., 2005. "Certainty-equivalence output-feedback design with circle-criterion observers". *IEEE*

- Transactions on Automatic Control, **50**(6), June, pp. 905–909.
- [56] Açıkmeşe, B., and Corless, M., 2011. "Observers for systems with nonlinearities satisfying incremental quadratic constraints". *Automatica*, **47**(7), pp. 1339 1348.
- [57] Lebastard, V., Aoustin, Y., Plestan, F., and Fridman, L., 2006. "Absolute orientation estimation based on high order sliding mode observer for a five link walking biped robot". In Variable Structure Systems, 2006. VSS'06. International Workshop on, pp. 373–378.
- [58] Lebastard, V., Aoustin, Y., and Plestan, F., 2006. "Observer-based control of a walking biped robot without orientation measurement". *Robotica*, **24**(3), May, pp. 385–400.
- [59] Lebastard, V., Aoustin, Y., and Plestan, F., 2005. "Stepby-step sliding mode observer for control of a walking biped robot by using only actuated variables measurement". In 2005 IEEE/RSJ International Conference on Intelligent Robots and Systems, pp. 559–564.
- [60] Grizzle, J. W., Choi, J. H., Hammouri, H., and Morris, B., 2007. "On observer-based feedback stabilization of periodic orbits in bipedal locomotion". In Methods and Models in Automation and Robotics, pp. 27–30.
- [61] Grizzle, J., Abba, G., and Plestan, F., 2001. "Asymptotically stable walking for biped robots: analysis via systems with impulse effects". *Automatic Control, IEEE Transactions on*, **46**(1), Jan, pp. 51–64.
- [62] Parker, T., and Chua, L., 1989. *Practical Numerical Algorithms for Chaotic Systems*. Springer.
- [63] Akbari Hamed, K., and Grizzle, J. W., 2017. "Reducedorder framework for exponential stabilization of periodic orbits on parameterized hybrid zero dynamics manifolds: Application to bipedal locomotion". Nonlinear Analysis: Hybrid Systems, 25, August, pp. 227– 245.
- [64] Buss, B., Akbari Hamed, K., Griffin, B. A., and Grizzle, J. W., 2016. "Experimental results for 3D bipedal robot walking based on systematic optimization of virtual constraints". In 2016 American Control Conference (ACC), pp. 4785–4792.
- [65] Dynamic Leg Locomotion YouTube Channel, 2015. MARLO: Dynamic 3D walking based on HZD gait design and BMI constraint selection, https://www.youtube.com/watch?v=5ms5DtPNwHo.
- [66] Hamed, K. A., Ames, A. D., and Gregg, R. D., 2018. "Observer-based feedback controllers for exponential stabilization of hybrid periodic orbits: Application to underactuated bipedal walking". In 2018 Annual American Control Conference (ACC), pp. 1438–1445.
- [67] Henrion, D., Lofberg, J., Kocvara, M., and Stingl, M., 2005. "Solving polynomial static output feedback problems with PENBMI". In Decision and Control, and European Control Conference. 44th IEEE Conference on, pp. 7581–7586.
- [68] de Oliveira, M., Bernussou, J., and Geromel, J., 1999. "A new discrete-time robust stability condition". *Systems & Control Letters*, **37**(4), pp. 261–265.

- [69] Toker, O., and Ozbay, H., 1995. "On the NP-hardness of solving bilinear matrix inequalities and simultaneous stabilization with static output feedback". In American Control Conference, Proceedings of the 1995, Vol. 4, pp. 2525–2526 vol.4.
- [70] de Leva, P., 1996. "Adjustments to Zatsiorsky-Seluyanov's segment inertia parameters". *J Biomech*, **29**(9), pp. 123–1230.
- [71] Maggiore, M., and Consolini, L., 2013. "Virtual holonomic constraints for Euler Lagrange systems". *Automatic Control, IEEE Transactions on*, **58**(4), April, pp. 1001–1008.
- [72] Mohammadi, A., Maggiore, M., and Consolini, L., 2018. "Dynamic virtual holonomic constraints for stabilization of closed orbits in underactuated mechanical systems". *Automatica*, **94**, pp. 112 124.
- [73] Hereid, A., Hubicki, C. M., Cousineau, E. A., and Ames, A. D., 2018. "Dynamic humanoid locomotion: A scalable formulation for HZD gait optimization". *IEEE Transactions on Robotics*, pp. 1–18.
- [74] Chevallereau, C., Grizzle, J., and Shih, C.-L., 2009. "Asymptotically stable walking of a five-link underactuated 3-D bipedal robot". *Robotics, IEEE Transactions on*, **25**(1), Feb, pp. 37–50.
- [75] TOMLAB optimization, http://tomopt.com/tomlab/.
- [76] Lofberg, J., 2004. "YALMIP: a toolbox for modeling and optimization in MATLAB". In Computer Aided Control Systems Design, 2004 IEEE International Symposium on, pp. 284–289.
- [77] Dynamic Output Controllers for Stabilization of Multi-Domain Robotic Locomotion, https://youtu. be/guKJK3DARas.
- [78] Shih, C.-L., Grizzle, J. W., and Chevallereau, C., 2012. "From stable walking to steering of a 3D bipedal robot with passive point feet". *Robotica*, **30**, 12, pp. 1119–1130.
- [79] Gregg, R., Tilton, A., Candido, S., Bretl, T., and Spong, M., 2012. "Control and planning of 3-D dynamic walking with asymptotically stable gait primitives". *Robotics, IEEE Transactions on*, **28**(6), Dec, pp. 1415–1423.
- [80] Gregg, R., and Righetti, L., 2013. "Controlled reduction with unactuated cyclic variables: Application to 3D bipedal walking with passive yaw rotation". Automatic Control, IEEE Transactions on, 58(10), Oct, pp. 2679–2685.
- [81] Dai, H., and Tedrake, R., 2013. "L₂-gain optimization for robust bipedal walking on unknown terrain". In Robotics and Automation, IEEE International Conference on, pp. 3116–3123.
- [82] Dai, H., and Tedrake, R., 2016. "Planning robust walking motion on uneven terrain via convex optimization". In 2016 IEEE-RAS 16th International Conference on Humanoid Robots (Humanoids), pp. 579–586.